



## STUDY OF ANTI-PROLIFERATIVE ACTIVITY OF PHENOLS FROM THE FRUIT RIND OF *M. MALABARICA*

Ajoy K. Bauri<sup>1\*</sup>, Ines Castro Diomicio<sup>2</sup>, Eric Salinas Arellano<sup>2</sup>, Sabine Foro<sup>3</sup> and Esperanza J. Carcache de Blanco<sup>2</sup>

<sup>1</sup>Bio-Organic Division, Bhabha Atomic Research Centre, Trombay, Mumbai 400085, India.

<sup>2</sup>College of Pharmacy, The Ohio State University, Ohio, Columbus, OH 43210, USA.

<sup>3</sup>Institute of Materials Science, Darmstadt University of Technology, Alarich-Weiss-Strasse 2, D-64287, Darmstadt, Germany.



\*Corresponding Author: Ajoy K. Bauri

Bio-Organic Division, Bhabha Atomic Research Centre, Trombay, Mumbai 400085, India.

Article Received on 21/05/2024

Article Revised on 11/06/2024

Article Accepted on 01/07/2024

### ABSTRACT

*M. malabarica* (family: Myristicaceae) is an Indian medicinal plant used as folklore medicine from very ancient time to cure various kind of diseases reported in Ayurved and fruit rinds are also used as an active ingredient for preparation of exotic spices known as 'garam masale'. Chemical profiling of methanol extract of defatted rind revealed the presence of a diarylnonanoids, a class of compounds generically known as malabaricones, as major constituents. Structural determination of these compounds has been conducted by physical, chemical, spectral, and spectrometric methods in comparison with spectroscopic data available in literature. In vitro assay of these compounds on various cancer cell lines revealed that they exhibited anti-proliferative activity using SRB assay.

**KEYWORDS:** *M. malabarica*; fruit rind; phenols; isolation and structural characterization; anti-proliferative activity; SRB assay.

### INTRODUCTION

The genus *Myristica* includes evergreen plants used as a folklore remedial agent to cure different kind of ailments, health care, health promoting purposes, as an active ingredient for preparation of exotic spices in various Indian cuisine.<sup>[1-3]</sup> *Myristica* is one of the twenty-one genera of Myristicaceae family and includes ten accepted species.<sup>[4]</sup> Most of them grow in the Eastern and Western Ghats Mountains of South India.<sup>[2,3]</sup> and in some parts of the Himalayan region.<sup>[5]</sup> The fruit rind, mace, and seeds are used as major ingredients in exotic spices, condiment, and as an active ingredient for formulations in Ayurveda, a traditional medicinal system of India. Thus, *M. malabarica* is the source of both nutmeg and mace.<sup>[6]</sup> Both of them are used as herbal medicine and as a spice.<sup>[3]</sup> Earlier chemical profiling of *M. malabarica* rind has revealed that the major active ingredients are diaryl nonanoids known as malabaricaone A-D.<sup>[7,8]</sup> while other *Myristica* species have yielded other class of compounds such as lignans,<sup>[9,10]</sup> resorcinol,<sup>[11]</sup> neolignans,<sup>[12-14]</sup> and isoflavonoids.<sup>[13]</sup> As part of ongoing study of bioactive natural products from *M. malabarica*, a more polar extract of the rind was investigated and yielded seven known malabaricones and related to them, one acyl phenol, and a substituted phenol called as

ericanone (8) along with other new phenolic derivatives with close resemblance to malabaricones and promalabaricones (10-12). The structure of these known compounds was identified by comparison with the <sup>1</sup>H NMR, <sup>13</sup>C NMR, 2D NMR and HRESI-MS data published in literature.<sup>[7,8]</sup> The efficacy of anti-proliferative activity of these compounds (1-14) has been screened against various human cancer cell lines by using SRB assay which is reported herein. Thus, this manuscript deals with the isolation of phenols, their structural characterization, and evaluation anti-proliferative activity of both known and unknown compounds from fruit rind of *M. malabarica*.

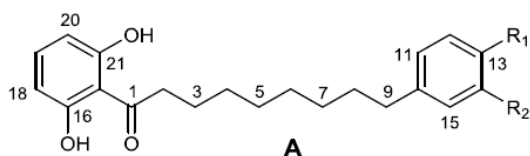
### RESULTS AND DISCUSSION

*M. malabarica* is a well-known herbal spice plant, widely distributed all over India especially in Eastern and Western Ghats Mountains. It is an evergreen tree and belongs to Myristicaceae family.<sup>[1-3]</sup> It has been recognised for its ethno-medicinal uses due to its high pharmacological potentials against various kind of ailments and as an active ingredient for preparation of exotic spices in Indian cuisine.<sup>[4-6]</sup> In local dialect, it is known as 'Masale Phool' ('Masala' means spice and 'Phool' means flower) and used in spice due to the

presence of its pleasant aroma. The dry fruit rind of *M. malabarica* has been used for extraction to investigate its chemical constituents. Initially, it was defatted with *n*-hexane, followed by extraction with methanol at room temperature. The solvent was removed to obtain a dark brown residue. This crude residue was fractionated by column chromatography over silica gel with gradient solvent elution by using a binary mixture of *n*-hexane-ethyl acetate followed by methanol-chloroform to yield several fractions, which were monitored by TLC. Fraction with similar TLC profiles were combined and, in some cases, further purified by column chromatography over silica gel, gel permeation chromatography (GPC), high performance liquid chromatography (HPLC) and preparative thin layer chromatography (PTLC) followed by crystallization to afford respective products. The UV absorption of these compounds very closely resembled with absorptions at 243 and 268 indicating presence of similar type of chromophore. Spraying with neutral  $\text{FeCl}_3$  solution (in

ethanol) on TLC plates showed dark green spots suggesting that these compounds were bearing a phenolic hydroxyl group adjacent to an acyl carbonyl group.<sup>[15, 16]</sup> These compounds also displayed batho-chromic shift in UV spectrum of about 35-40 nm upon the addition of anhydrous  $\text{AlCl}_3$  due to formation six-member complex which is stable in acidic medium.<sup>[17]</sup> This complexation with  $\text{AlCl}_3$  indicated that the presence of 3-hydroxy ketone moiety in these compounds.<sup>[17]</sup>  $^1\text{H}$  NMR spectra with mass spectral fragments arising from acyl cleavage provided a clear indication of the nature and substitution pattern of benzene rings in nonanoids and their analogues.<sup>[7]</sup>

Compounds 1-4 and 14 were identified as malabaricones A-D (Figure 1A) and carboxy malabaricone B by comparison of their spectroscopic data with those published for the previously identified compounds.<sup>[7]</sup> The ORTEP diagram of malabaricones A and C is shown below (Figures 1B-C).



- (i)  $\text{R}_1 = \text{R}_2 = \text{H}$ ; Malabaricone A (1)
- (ii)  $\text{R}_1 = \text{OH}$  &  $\text{R}_2 = \text{H}$ ; Malabaricone B (2)
- (iii)  $\text{R}_1 = \text{R}_2 = \text{OH}$ ; Malabaricone C (3)
- (iv)  $\text{R}_1, \text{R}_2 = -\text{O}-\text{CH}_2-\text{O}-$ ; Malabaricone D (4)
- (v)  $\text{R}_1 = \text{OH}$  &  $\text{R}_2 = \text{COOH}$ ; Carboxy-malabaricone B (14)

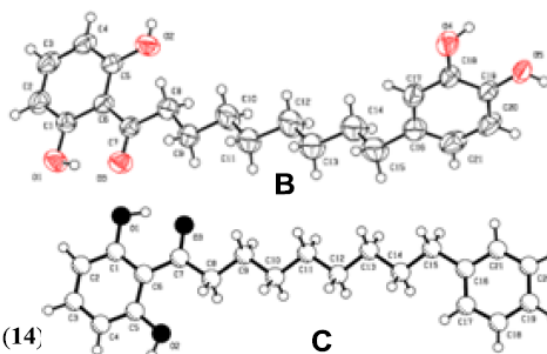
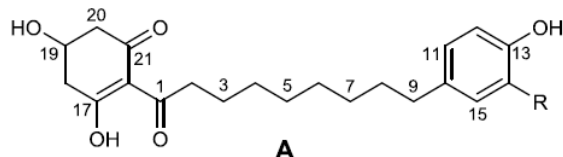


**Figure 1A-1C: Structures of malabaricones A-D (1-4 & 14), ORTEP diagram of malabaricones C & A** Previously the anti-proliferative activities of these malabaricones have been evaluated on various cancer cell lines and some of them had significant anti-proliferative activity on specific cell lines.<sup>[18-27]</sup>

Compounds 5 and 6 (Figure 2A) were also identified as promalabaricones B and C by comparison of their spectroscopic data with those of the known compounds previously isolated from *M. maingayi*<sup>[28]</sup> a tropical tree

of the *Myristica* genus occurring in Malaysia and Vietnam. This is the first report of these compounds from *M. malabarica* available in Eastern and Western Ghats Mountains in India.



- (vi).  $\text{R} = \text{H}$ ; Promalabaricone B (5)
- (vii).  $\text{R} = \text{OH}$ ; Promalabaricone C (6)

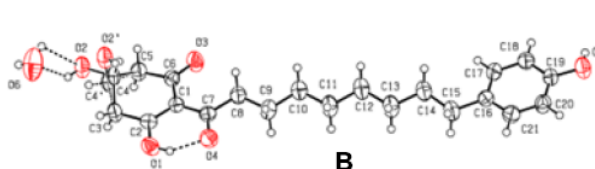
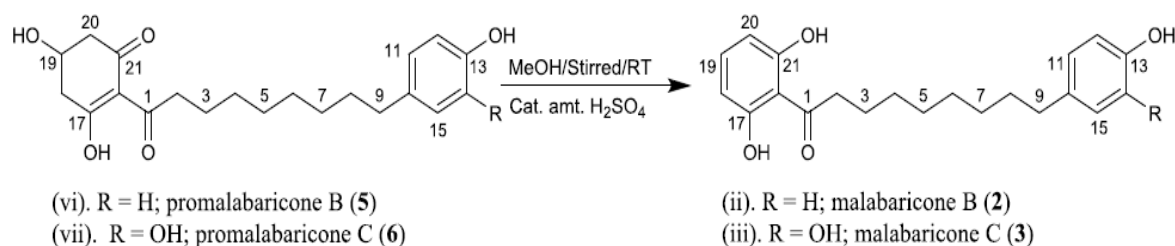


**Figure 2A-2B: Structures of compounds (5) and (6) & ORTEP diagram of promalabaricone B** Confirmation of structures of compounds 5 and 6 was obtained by their chemical conversion into malabaricone B and malabaricone C on stirring overnight in methanol in presence of catalytic amount  $\text{H}_2\text{SO}_4$  at room temperature.<sup>[29]</sup>

The 3, 5 dihydroxycyclohexenyl-one moieties underwent dehydration and subsequent aromatization to form 2, 6 dihydroxyphenyl rings of malabaricone B and

malabaricone C depicted in scheme 1. The crystal for the structure of compound 5 is also provided in Figure 2B.



**Scheme 1: Conversion of promalabaricones (5, 6) to malabaricones (2, 3).**

Compound 7 was isolated as light pale-yellow needles with the molecular formula  $C_{20}H_{32}O_3$  established by HRESI in negative mode with  $m/z$  319.2275  $[M-H]^-$  (observed  $m/z$  319.2275 and calculated  $m/z$  319.2273) in combination with the  $^1H$  and  $^{13}C$  NMR spectra. Its structure was defined as 1-(2,6-dihydroxyphenyl) tetradecane-1-one based on its NMR and mass spectra, and by comparison with the literature data.<sup>[30,31]</sup> Compound 7 is significantly more potent than the similar

compound thouvenol A or (Z)-1-(2, 4, 6-trihydroxyphenyl) octadecane-13-ene-1-one performed on cell line A2780.<sup>[32,33]</sup> It is not clear whether this difference is due to the length of the side chain or to the number and position number of phenolic hydroxyl groups. The structure of compound 7 was confirmed by X-ray diffraction study (see Figure 5 and supporting information in Annexure-1). The ORTEP diagram of compound 7 is also provided in figure 3B.

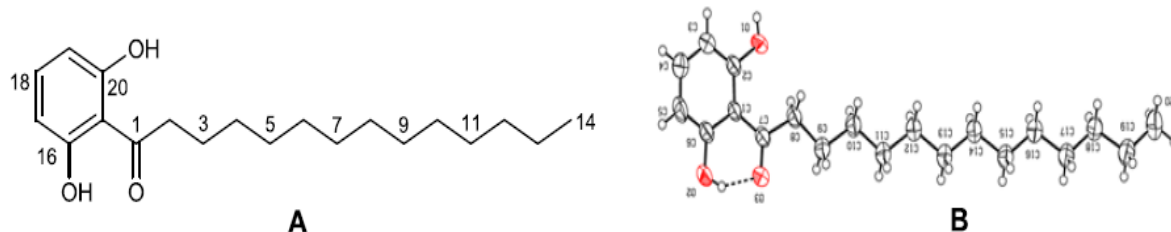


**Figure 3A-3B: Structures of Acyl phenol (7) & ORTEP diagram of Acyl phenol (7).**

Compound 8 isolated as pale-yellow amorphous solid with the molecular formula  $C_{20}H_{32}O_3$  established by HRESI in positive mode at  $m/z$  359.1838  $[M+H]^+$  (observed  $m/z$  359.1838 and calculated  $m/z$  359.1858) in combination with the  $^1H$  and  $^{13}C$  NMR spectra. It had

been assigned as ericanone, and this is the first report of this compound from *M. malabarica*.<sup>[34]</sup> Earlier, it has been reported from *Erica cinerea* plant.<sup>[29]</sup> The structure of compound is depicted below in figure 4.

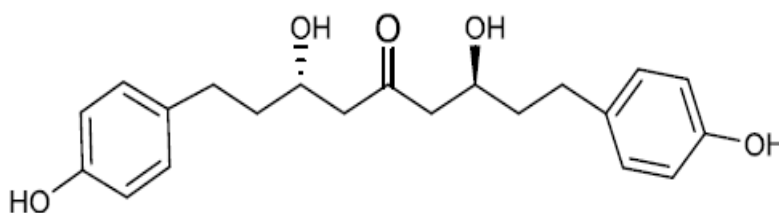


**Figure 4: Structure of ericanone (8).**

Compound 9 (Hydrated malabaricone C) isolated as colourless needle shaped crystal with the molecular formula  $C_{20}H_{32}O_3$  established by HRESI mass in positive mode at  $m/z$  359.1838  $[M+H]^+$  and 381.1657  $[M+Na]^+$  (observed  $m/z$  359.1858 and calculated  $m/z$  381.1678) in combination with the  $^1H$  and  $^{13}C$  NMR spectra. It was a hydrolysed product of more polar fraction to obtain from aqueous methanol extract on acid hydrolysis of black mug substance followed by usual worked up and

assigned as hydrated malabaricone C. Its melting point differed in about 20 °C. Chemical shift values have been observed in the NMR spectrum, mass values have been gathered, splitting pattern and chemical shift values showed slight variations in comparison to  $^1H$  and  $^{13}C$  NMR spectrum of compound 3 (malabaricone C), as mentioned in Table 2 and 3 and supplementary information (Annexure 1). There are very marginal differences in  $^1H$  NMR and  $^{13}C$  NMR spectrum of

compound 4 and compound except XRD structure and melting point. Furthermore, it has been confirmed by a single crystal X-ray diffraction study (please see SI in

Annexure 1). The structure and ORTEP diagram of compound 9 is depicted below in Figure 5A and Figure 5B.

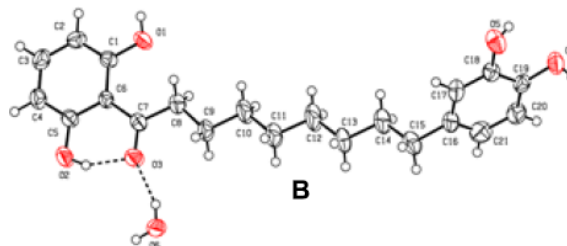
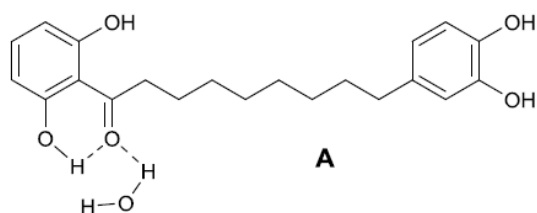
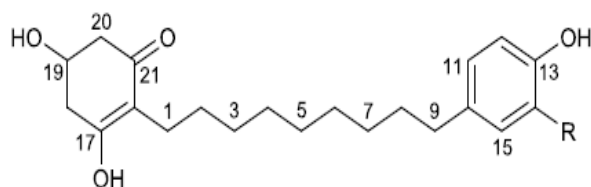


**Figure 5A-5B: Structure of hydrated malabaricone C (9) & ORTEP of hydrated malabaricone C (9).**

Compounds 10 and 11 were also identified as a derivative of promalabaricones B and C known as promalabaricone. The structural skeletons of compounds 10 and 11 are very similar to promalabaricones B and C (5 & 6) except one carbonyl group in nonanoid chain. Therefore, compounds 10 and 11 are flanking with two rings, cyclohexenyl and aryl with different substituent at

the terminal positions by means of nonanyl chain that is why it is called as promalabaricone. The structure of the compounds 10 and 11 has been determined by chemical, spectral and spectrometric methods. These are new compounds and reported first time from *Myristica* species. The structure of compounds 10 and 11 have been determined as depicted below in Figure 6.



R = H; Derivative of Promalabaricone B (10)  
R = OH; Derivative of Promalabaricone C (11)

**Figure 6: Structure of compound 10 & compound 11.**

Compound 12 (carboxymalabaricone B) isolated as colourless needle shaped crystal (mp. 106-107 °C) with the molecular formula  $C_{21}H_{32}O_3$  established by HRESI mass in positive mode at  $m/z$  359.1838  $[M+H-CO_2]^+$  and 381.1657  $[M+Na]^+$  (observed  $m/z$  359.1858 and calculated  $m/z$  381.1678) in combination with the  $^1H$  and  $^{13}C$  NMR spectra. It was a hydrolysed product of more polar fraction to obtain from aqueous methanol extract on acid hydrolysis of black mug substance followed by usual worked up and assigned as hydrated malabaricone

C. Its melting point differed in about 20 °C. Chemical shift values have been observed in the NMR spectrum, mass values have been gathered, splitting pattern and chemical shift values showed slight variations on comparison to  $^1H$  and  $^{13}C$  NMR spectrum of compound 3 (malabaricone C), as mentioned in Table 2 & 3 and supplementary information. This compound is also reported first time from *Myristica* species. The structure of compound 12 has been determined as depicted below in Figure 7.

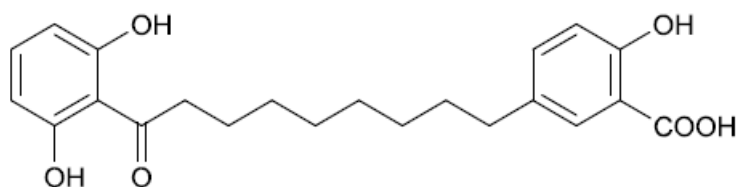


**Figure 7: Structure of carboxy malabaricone B (12).**

In a literature survey, it was found that all plants of *Myristica* species did not biosynthesize malabaricones although they are belonging to same family Myristicaceae. It was also found that some of the species of the *Myristica* plants such as *M. alba*,<sup>[34]</sup> *M. andamanica*,<sup>[16]</sup> *M. argentea*,<sup>[8,35]</sup> *M. maxima*,<sup>[34,36]</sup> *M.*

*swamps*,<sup>[34,36]</sup> *M. astrescens*,<sup>[37,38]</sup> *M. basilanica*,<sup>[35,38]</sup> *M. brachipoda*,<sup>[26,38]</sup> *M. brevistipes*,<sup>[28,34,39]</sup> *M. fragrans*,<sup>[28,30,31,37-47]</sup> *M. maingayi*,<sup>[48-50]</sup> *M. beddomei*,<sup>[1,28,39]</sup> *M. fatua*,<sup>[36,51,52]</sup> *M. magnifica*,<sup>[29,34]</sup> and *M. philippensis*,<sup>[53,29]</sup> did not biosynthesize malabaricones. But, malabaricone C and its dimer known



as gigantone has been reported from *M. cinnamomea*, a *Myristica* plant available in Malaysia.<sup>[54-56]</sup> However, the main credential of these medicinal plants is that the majority of Asian population relies on these plants for their primary healthcare and health promoting purposes.

## CONCLUSION

Fruit rind is an iconic spice and condiment in Indian cuisine. Twelve phenolic compounds 1-12 were isolated from defatted methanol extract of fruit rind of *M. malabarica*. The structural determination of known compounds has been identified by chemical, spectral and spectrometric methods in comparison with the spectral data available in literature. The efficacy of anti-proliferative activity has been examined on five different types of human cancer cell lines including urinary bladder (HT-1376), pancreatic (HPAC), prostate (DU-145), colon (HT-29) and thyroid (MDA-T32). Cell cytotoxicity study has been performed by using SRB assay in comparison to paclitaxel as control. Experimental results revealed that all compounds had anti-proliferative activity at the concentration of microgram ( $\mu\text{g}$ ) level, by considering active those compounds exhibiting IC<sub>50</sub> values below 50  $\mu\text{g/mL}$ . It was found that compounds 5 and 6 were active on cell line HT-1376 while, other compounds exhibited anti-proliferative activity in the range of IC<sub>50</sub> values 22.16-31.66  $\mu\text{g/mL}$ . Compounds 1-9 inhibited proliferation on HPAC cell line as listed in Table 1 in the range of IC<sub>50</sub> values between 15-24  $\mu\text{g/mL}$ . All compounds had negligible anti-proliferative activity against cell line DU-145 except compound 4, which exhibited IC<sub>50</sub> values 18.75  $\mu\text{g/mL}$ . Compounds 4 and 7 possess anti-proliferative activity with IC<sub>50</sub> values of 30.95  $\mu\text{g/mL}$  and 19.18  $\mu\text{g/mL}$  on HT-29 cell line, respectively. Anti-proliferative activity of the compound 1 and 2 was <50 ( $21.58 \pm 2.1$ ) and <50 ( $15.77 \pm 1.8$ ) against MDA-T32 cell line, whereas the remaining compounds except 10-12 exhibited activity in the range of IC<sub>50</sub> values 15.54-27.55  $\mu\text{g/mL}$ .

## Experimental section

### General experimental procedures

Melting points were determined using a Buchi M560 (Switzerland) melting point apparatus. Specific rotations were obtained using a JASCO DIP 1000 digital polarimeter. UV spectra were measured on Shimadzu UV-2100 UV-Vis spectrophotometer. NMR spectra were recorded in CDCl<sub>3</sub> or CD<sub>3</sub>OD on a Bruker Avance 200, NOVA-400, Varian 500 AR and Varian 800 spectrometer using residual CHCl<sub>3</sub>/H<sub>2</sub>O as an internal standard. Chemical shifts are given in ppm ( $\delta\text{C}$  &  $\delta\text{H}$ ), relative to residue CHCl<sub>3</sub>/H<sub>2</sub>O (7.25 & 77.00/4.78 or 3.30 & 49.00 ppm). Mass spectra (EI) were registered using Fission 8000 (8000 series, UK) and Shimadzu QP5050A mass spectrometer, Japan. UHPLC/MS analysis of the samples was performed using a Vanquish UHPLC system coupled to a Q-Exactive quadrupole orbitrap mass spectrometer (Thermo Fisher Scientific, USA) at College of Pharmacy Instrumentation Facility, The Ohio State

University. Crystal data were collected at 293 °K on an Oxford Diffraction Xcalibur™ Single Crystal X-ray Diffractometer with Sapphire CCD Detector, Enhance (Mo) or Cu-K $\alpha$  X-ray source, and graphite monochromator using  $\omega$  scans. The structures were solved by direct methods and refined using SHELXL97. Silica gel 60 (230-400 mesh, Merck) was used for analytical TLC. Silica gel 60 (70-230 mesh, Merck) was used for column chromatography. All compounds were visualized by TLC using vanillin-perchloric acid-EtOH followed by heating at 110 °C for 5 min, DNP in EtOH and neutral FeCl<sub>3</sub> in MeOH.

**Anti-proliferative bioassay.** Evaluation of anti-proliferative activity of malabaricones and their homologues against different cancer cell lines by using sulfo-rhodamine B assay was performed at College of Pharmacy, The Ohio State University, Ohio, Columbus, USA.<sup>[57-60]</sup>

**Sample preparation.** Test samples and controls (paclitaxel) were dissolved in 100% DMSO to prepare stock solutions of 10 mg/mL. Dilutions were prepared using 10% DMSO in water and 100% water.

**Cell culture.** Cancer cells [urinary bladder (HT-1376), pancreatic (HPAC), prostate (DU-145), colon (HT-29) and thyroid (MDA-T32)] were obtained from American Type Culture Collection, Manassas, VA, USA. Monolayer cells were cultured using T75 tissue culture flasks in Roswell Park Memorial Institute medium (RPMI) or Dulbecco's Modified Eagle Medium (DMEM), containing 10% fetal bovine serum and 1% antibiotic-anti-mycotic from Gibco. Cells were kept at 37 °C and in an atmosphere with 5% of CO<sub>2</sub>.

**Anti-proliferative assays.** Anti-proliferative activity of test samples was evaluated in triplicate on cancer cells, using a sulforhodamine B (SRB) assay as reported previously, in three independent experiments.<sup>[59,60]</sup>

### Plant material

The spice *M. malabarica* was purchased in a local market in Mumbai in May, 2019. The material was authenticated by Dr. Hussain Barbhuiya, Landscape and Cosmetic Maintenance Section, A & SED Division, Bhabha Atomic Research Centre, Trombay, Mumbai. A voucher specimen was deposited in the Herbarium of the Landscape & Cosmetic Maintenance Division, BARC, Mumbai-400085 having accession number HBARC00006631.

### Extraction and Isolation

Fresh quality fruit rind (1.250 Kg) of *M. malabarica* were dried and ground to a powder, which was extracted with methanol (2.5 L) three times at room temperature. Removal of solvent by using rota-vapour maintaining water bath temperature at 40 °C afforded a brown viscous residue (~370 g). This extract was fractionated over silica gel (5.0 kg, 230-400 mesh, Aldrich) and

eluted with a step gradient of hexane, ethyl acetate in hexane, then chloroform and mixtures of methanol in chloroform to furnish one hundred fractions having volume of each aliquot was approximately 500-1000 mL. In some cases, the volume of aliquot collected is more than 1000 mL. Fractions were monitored by TLC to examine the chemical profiles. The fractions having similar chemical profiles were combined together and, in some cases, further purified by using repetitive column chromatography on open column chromatography over silica gel, gel permeation chromatography (GPC) with solvent gradual elution followed by preparative thin layer chromatography (PTLC).

Fractions 1-8 eluted with hexane to ethyl acetate (0-15%) consisted mainly of traces amount of lipids.

Fractions 9-11 eluted with chloroform-methanol (0-5%) contained fatty acids along with a phenolic compound. On evaporation yielded residue A (~150 mg), which was subjected to gel permeation chromatography (GPC) over a sephadexLH-20 column eluted with chloroform-methanol (5-10%) in a step gradient to yield five sub-fractions A1-A5. Chromatography separation of sub-fractions A3-A4 on a silica gel open column gave compound 7 (~112 mg). Fractions 12-13 eluted by a mixture of chloroform-methanol (5%) were combined and evaporated to furnish the pale-yellow residue B (1.05 g). This was further chromatography sequentially over silica gel and then over sephadexLH-20 column eluted with 10% methanol in chloroform to yield sub-fractions B1-B10. Sub-fractions B5-B7 was monitored by TLC and performed chemical study with various spray reagent. It observed that sub-fractions B5-B7 were similar chemical profiles. They were combined (~1.2 g) and separated on a silica gel open column to afford compound 1 (~1.0 g) designated as malabaricone A.

Fractions 14-22 eluted by a mixture of chloroform-methanol (7%) were combined and evaporated to furnish a yellowish residue C (1.5 gm). This was further chromatography sequentially over silica gel and then over sephadexLH-20 column eluted with 10% methanol in chloroform to yield sub-fractions C1-C15. Sub-fractions C5-C10 was monitored by TLC and performed chemical study with various spray reagents. It was observed that sub-fractions C5-C10 were similar chemical profiles. They were combined (~1.2 gm) and separated on a silica gel open column to afford compound 4 (~1.1 gm), assigned as malabaricone D.

Fractions 23-33 obtained from elution with 7-10% methanol in chloroform were combined and evaporated to afford residue (2.0 gm).

Fractions 34-42 eluted with 10% methanol in chloroform were combined and evaporated to yield residue (~ 3.5 gm). These residues were monitored by TLC. Chemical profiles of these residues on TLC were similar and they were combined together. The combined residue, D (~ 5.5

gm) was chromatography on a sephadexLH-20 column eluted with chloroform-methanol (0-100%) to yield thirty-five sub-fractions D1-D35. Sub-fractions D7-D25 were combined on the basis of TLC profiles to yield a residue (~ 5.0 gm) which was separated by open column chromatography over silica gel to yield compound 2 (~ 4.5 gm) compound designated as malabaricone B.

Column fractions 43-59 eluted with 10-15% methanol in chloroform had similar TLC profiles and were combined an evaporate to give product, E (13.0 gm) which was purified by chromatography on a sephadexLH-20 column eluted with a gradient of chloroform to methanol (0-100%) to yield twenty-five sub-fractions E1-E25. Sub-fractions E7-E12 (~12.5 g) had similar TLC profiles and were combined and separated on a silica gel open column eluted with a step gradient of chloroform-methanol to yield compound 3 (~11.5 g) assigned as malabaricone C, which was a major constituent in this extract.

Fractions 60-70 eluted with 15% methanol in chloroform were combined to give a residue F (300 mg), which was separated on a sephadexLH-20 column eluted with chloroform-methanol (0-100%) to give ten sub-fractions F1-F10. Sub-fractions F4-F5 were combined and evaporated to furnish brown residue. This residue was repetitive chromatography over a silica gel on open column followed by preparative TLC to yield compound 8 (~150 mg) assigned as ericanone.

Fractions 71-80 eluted with 20% methanol in chloroform were combined to give a residue G (100 mg) which was separated on a sephadexLH-20 column eluted with chloroform-methanol (0-100%) to give ten sub-fractions G1-G10. Sub-fractions G4-G5 were combined and evaporated to furnish an off-white residue. This residue was subjected to repetitive chromatography over a silica gel on open column followed by preparative TLC to yield compounds 5 (~25 mg) assigned as promalabaricone B and 6 (14.0 mg) assigned as promalabaricone C.

Fractions 81-86 eluted with 20-25% methanol in chloroform were combined to give a residue H (150 mg) which was separated on a sephadexLH-20 column eluted with chloroform-methanol (0-100%) to give ten sub-fractions H1-H10. Sub-fractions H5-H7 were combined and evaporated to obtain a brown residue. This residue was repetitive chromatographed over a silica gel on open column followed by preparative TLC to yield compounds compound 5a and 6a (120 mg). The structural skeleton of these compounds was very similar to compounds 5 and 6 except functionalities based on assignment of spectral studies. The structure of compounds 5a and 6a has been assigned as depicted below in Figure 7.

Fractions 87-93 eluted with 30% methanol in chloroform were combined to give a residue I (500 mg) which was separated on a sephadexLH-20 column eluted with chloroform-methanol (0-100%) to give twelve sub-fractions I1-I12. Sub-fractions I3-I5 were combined and evaporated to furnish a light brown residue. This residue was repetitive chromatography over a silica gel on open column followed by preparative TLC to yield a mixture compound (200 mg). The analysis of crude products was not done.

Fractions 94-97 eluted with 35% methanol in chloroform were combined to give a residue J (~50 gm). It appeared as black sticky mass highly hygroscopic in nature. About 1.0 gm of residue J was acid hydrolysed (2N aqueous HCl) for one hour in a water bath. The hydrolysed product was worked up by usual method to afford a light brown residue JJ (~ 400 mg). This residue was monitored by TLC using 10% methanol in chloroform as solvent system and visualized on exposure in UV light. It observed that one major spot along with other three very minor spots in micro plate. This residue was purified on a sephadexLH-20 column eluted with chloroform-methanol (0-100%) to collect eight sub-fractions JJ1-JJ8. Sub-fractions JJ4-JJ5 were combined based on their TLC profiles and evaporated to furnish an off-white residue (~ 300 mg). This residue was repetitive chromatography over a silica gel on open column, preparative TLC followed by crystallization to yield a needle shaped colourless crystalline compound assigned as compound **9** (250 mg) along with minor constituent **14** (approximately 25 mg). The compound **9** was identified as hydrated malabaricone C by spectroscopic study and confirmed by single crystal XRD study. The structure of compound **14** has been determined as carboxy malabaricone B in comparison with <sup>1</sup>H & <sup>13</sup>C NMR data of malabaricone B.

The aqueous part contained sugars. The sugar moiety presents in the aqueous part was identified as D (+) glucose on comparison with authentic sugar D (+) glucose. So, majority of black sticky mass is glycoside of malabaricone C along with other compounds in very trace amount, but determination of number sugar moiety and attachment of sugar moiety (s) into this aglycone has been undetermined.

Fractions 98-100 eluted with 50-100% methanol in chloroform were combined to give a mug substance K (~ 100 gm). It appeared as black sticky mass, highly hygroscopic in nature. It looks like polyphenolic compounds in the form of glycosides or complex polysaccharide of the above secondary metabolites. Further investigation of this fraction has not been done.

Compound **1** (malabaricone A): yellow prisms (EtOAc-Hexane); mp. 82°C; UV (MeOH)  $\lambda_{max}$  (log  $\epsilon$ ): 206 (1.305), 268 (0.752), 340 (0.198) nm; IR (KBr)  $\nu_{max}$ : 3465, 3390, 3259, 2998 and 1625 cm<sup>-1</sup>; HRESI-MS (negative mode): obs.  $m/z$  value 323.1898 au [M-H]<sup>-</sup> ;

cal.  $m/z$  value 323.191 au [M-H]<sup>-</sup>. <sup>1</sup>H NMR (CD<sub>3</sub>OD, 200 MHz) and <sup>13</sup>C NMR (CD<sub>3</sub>OD, 50 MHz) see Table 23. CCDC reference number: 605059. <https://doi.org/10.1107/S1600536806008257>

Compound **2** (malabaricone B): colourless needles (EtOAc-Hexane); mp. 98 °C; UV (MeOH)  $\lambda_{max}$  (log  $\epsilon$ ): 224 (0.614), 270 (0.334), 346 (0.198) nm; IR (KBr)  $\nu_{max}$ : 3464, 3390, 3259, 2985, 1626 cm<sup>-1</sup>; HR-ESI (positive mode)  $m/z$ : 341.1740 Da [M + H]<sup>+</sup>. <sup>1</sup>H NMR (CD<sub>3</sub>OD, 200 MHz) and <sup>13</sup>C NMR (CD<sub>3</sub>OD, 50 MHz) data, see Table 2. CCDC reference number: 2212418

Compound **3** (malabaricone C): Dark yellow needles (CHCl<sub>3</sub>-MeOH); mp. 120 °C; UV (MeOH)  $\lambda_{max}$  (log  $\epsilon$ ): 206 (1.665), 270 (0.885), 342 (0.210) nm; IR (KBr)  $\nu_{max}$ : 3468, 3392, 3259, 2987 and 1628 cm<sup>-1</sup>; HRESI-MS (positive mode),  $m/z$ : 359.1844Da [M+ H]<sup>+</sup> & 379.1506 Da [M+H<sub>2</sub>O]<sup>+</sup>. <sup>1</sup>H NMR (CD<sub>3</sub>OD, 200 MHz) and <sup>13</sup>C NMR (CD<sub>3</sub>OD, 50 MHz) see Table 2. CCDC reference number:610702. Crystal structure and crystal data of compound **2** can be accessed using site: <https://doi.org/10.1107/S1600536806015273>

Compound **4** (malabaricone D): colourless rods (MeOH); mp. 90 °C; UV (MeOH)  $\lambda_{max}$  (log  $\epsilon$ ): 228 (4.040), 268 (4.125), 342 (1.077) nm; IR (KBr)  $\nu_{max}$ : 3467.50, 3387.15, 3257.05, 2898.25 and 1628.45 cm<sup>-1</sup>; <sup>1</sup>H NMR (CD<sub>3</sub>OD, 200 MHz) and <sup>13</sup>C NMR (CD<sub>3</sub>OD, 50 MHz) data, see Table 2; HR-ESI (positive mode)  $m/z$ : 371.1834 Da [M+H]<sup>+</sup> and 393.1662 Da [M + Na]<sup>+</sup>. <sup>1</sup>H NMR (CD<sub>3</sub>OD, 200 MHz) and <sup>13</sup>C NMR (CD<sub>3</sub>OD, 50 MHz) see Table 2. CCDC reference number: 2212500.

Compound **5** (promalabaricone B): colourless needles; mp. 141-142 °C; UV (MeOH)  $\lambda_{max}$  (log  $\epsilon$ ): 274 (3.2), 228 (3.8); IR (KBr)  $\nu_{max}$ : 3340.1, 2918.7, 2848.4, 1737.6, 1633.4, 1585.2, 1512.8, 1447.3, 1366.2, 1245.7, 1036.5, 825.3, 781.9, 717.4 cm<sup>-1</sup>; <sup>1</sup>H NMR (CD<sub>3</sub>OD, 200 MHz) and <sup>13</sup>C NMR (CD<sub>3</sub>OD, 50 MHz) data, see Table 2. HRESI-MS (positive mode)  $m/z$ : 361.1990 Da [M+ H]<sup>+</sup>; <sup>1</sup>H NMR (CD<sub>3</sub>OD, 200 MHz) and <sup>13</sup>C NMR (CD<sub>3</sub>OD, 50 MHz) see Table 3. CCDC reference number:1501296. Crystal structure and crystal data of compound **5** can be accessed using site: <https://doi.org/10.1107/S2056989016013797>

Compound **6** (promalabaricone C): colourless needles (EtOAc-Hexane); mp.149-150 °C; UV (MeOH)  $\lambda_{max}$ : 274 (3.2), 228 (3.8); IR (KBr)  $\nu_{max}$ : 3340.1, 2918.7, 2848.4, 1737.6, 1633.4, 1585.2; 1512.8, 1447.3, 1366.2, 1245.7, 1036.5, 825.3, 781.9, 717.4 cm<sup>-1</sup>; HR-ESI (positive mode)  $m/z$ : 361.1976 Da [M+H]<sup>+</sup> & 383.1813 Da [M+Na]<sup>+</sup>. <sup>1</sup>H NMR (CD<sub>3</sub>OD, 200 MHz) and <sup>13</sup>C NMR (CD<sub>3</sub>OD, 50 MHz) see Table 3.

Compound **7** [1-(2',6'-dihydroxyphenyl)-tetradecan-1-one]: colourless needles (EtOAc-Hexane); mp. 90 °C. IR (KBr)  $\nu_{max}$ : 3466, 3392, 3258, 2985 and 1628 cm<sup>-1</sup>;

UV (MeOH)  $\lambda_{max}$  (log  $\epsilon$ ): 222 (0.906), 268 (0.785), 340 (0.205) nm; HRESI (negative mode)  $m/z$ : 319.2275 Da [M-H]<sup>-</sup> and 639.4630 [2M-H]<sup>-</sup>, dimerization. 1H NMR (CD<sub>3</sub>OD, 200 MHz) and 13C NMR (CD<sub>3</sub>OD, 50 MHz) see Table 3. CCDC reference number: 1591296

Compound **8** [1-(3,7-dihydroxy-1,9-bis(4-hydroxyphenyl)-nonan-5-one]: light brown amorphous substance (EtOAc-Hexane); mp. 147-150 °C. IR (KBr)  $\nu_{max}$ : 3303, 2915, 2850, 1569, 1514, 1361, 12224, 1041, 851, 818 and 722 and 1628 cm<sup>-1</sup>; UV (MeOH),  $\lambda_{max}$ : 204, 223, 237 nm; HRESI  $m/z$ : 359.1838 Da [M+H]<sup>+</sup> & 381.1656 Da [M+Na]<sup>+</sup>. 1H NMR (CD<sub>3</sub>OD, 200 MHz) and 13C NMR (CD<sub>3</sub>OD, 50 MHz) see Table 3.

Compound **9** (Hydrated malabaricone C): colourless needles (CHCl<sub>3</sub>-MeOH); mp. 122 °C; UV (MeOH)  $\lambda_{max}$  (log  $\epsilon$ ): 206 (1.665), 270 (0.885), 342 (0.210) nm; IR (KBr)  $\nu_{max}$ : 3468, 3392, 3259, 2987 and 1628 cm<sup>-1</sup>; 1H NMR (CD<sub>3</sub>OD, 200 MHz) and 13C NMR (CD<sub>3</sub>OD, 50 MHz) data see Table 2; HR-ESI (positive mode)  $m/z$ : 359.1837 Da [M + H]<sup>+</sup> & 381.1657 Da [M + Na]<sup>+</sup>. 1H NMR (CD<sub>3</sub>OD, 200 MHz) and 13C NMR (CD<sub>3</sub>OD, 50 MHz) see Table 3.

Compound **10** (Promalabaricane B, linker is nonane chain. No carbonyl in aliphatic chain): colourless

needles; mp. 150-152 °C; UV (MeOH)  $\lambda_{max}$  (log  $\epsilon$ ): 274 (3.2), 228 (3.8); IR (KBr)  $\nu_{max}$ : 3340.1, 2918.7, 2848.4, 1737.6, 1633.4, 1585.2, 1512.8, 1447.3, 1366.2, 1245.7, 1036.5, 825.3, 781.9, 717.4 cm<sup>-1</sup>; 1H NMR (CD<sub>3</sub>OD, 200 MHz) and 13C NMR (CD<sub>3</sub>OD, 50 MHz) data, see Table 2. HR-ESI (positive mode)  $m/z$ : 361.1990 Da [M+H]<sup>+</sup>; 1H NMR (CD<sub>3</sub>OD, 200 MHz) and 13C NMR (CD<sub>3</sub>OD, 50 MHz) see Table 4.

Compound **11** (Promalabaricane C, linker is nonane chain. No carbonyl in aliphatic chain): colourless needles (EtOAc-Hexane); mp. 149-150 °C; UV (MeOH)  $\lambda_{max}$ : 274 (3.2), 228 (3.8); IR (KBr)  $\nu_{max}$ : 3340.1, 2918.7, 2848.4, 1737.6, 1633.4, 1585.2; 1512.8, 1447.3, 1366.2, 1245.7, 1036.5, 825.3, 781.9, 717.4 cm<sup>-1</sup>; HRESI (positive mode)  $m/z$ : 361.1976 Da [M+H]<sup>+</sup> & 383.1813 Da [M+Na]<sup>+</sup>. 1H NMR (CD<sub>3</sub>OD, 200 MHz) and 13C NMR (CD<sub>3</sub>OD, 50 MHz) see Table 3.

Compound **12** (Carboxy-malabaricone B): colourless needles (EtOAc-Hexane); mp. 106-107 °C; UV (MeOH)  $\lambda_{max}$ : 274 (3.2), 228 (3.8); IR (KBr)  $\nu_{max}$ : 3343.1, 2918.7, 2845.4, 1733.6, 1635.4, 1581.2; 1515.8, 1447.3, 1366.2, 1245.7, 1036.5, 825.3, 781.9, 717.4 cm<sup>-1</sup>; HR-ESI (positive mode)  $m/z$ : 361.1976 Da [M+H]<sup>+</sup> & 383.1813 Da [M+Na]<sup>+</sup>. 1H NMR (CD<sub>3</sub>OD, 200 MHz) and 13C NMR (CD<sub>3</sub>OD, 50 MHz) see Table 4.

**Table 1: Anti-proliferative activity of malabaricones and their analogues against different cancer cell lines by using sulforhodamine B (SRB) assay.**

Sample	Name of five types cancer cell lines used forevaluation of anti-proliferative activity in compare to paclitaxel as control by using (SRB) assay									
	HT-1376 (Urinary bladder)		HPAC (Pancreatic)		DU-145 (Prostate)		HT-29 (Colon)		MDA-T32 (Thyroid)	
	% Inhibition ± SE	IC <sub>50</sub> ± SE	% Inhibition ± SE	IC <sub>50</sub> ± SE	% Inhibition ± SE	IC <sub>50</sub> ± SE	% Inhibition ± SE	IC <sub>50</sub> ± SE	% Inhibition ± SE	IC <sub>50</sub> ± SE
1	49.32 ± 2.7	31.66 ± 8.3	69.37 ± 1.0	16.50 ± 3.3	<50 (2.45 ± 3.9)	-	<50 (21.58 ± 2.1)	-	<50 (15.77 ± 1.8)	-
2	42.62 ± 2.6	33.01 ± 4.2	70.17 ± 0.6	15.06 ± 2.7	<50 (30.06 ± 2.8)	-	<50 (24.61 ± 7.6)	-	<50 (39.46 ± 2.3)	-
3	45.62 ± 1.6	23.11 ± 3.1	69.73 ± 0.9	15.73 ± 3.0	<50 (18.68 ± 1.9)	-	<50 (8.50 ± 1.4)	-	47.69 ± 1.1	26.83 ± 2.8
4	53.50 ± 1.3	25.21 ± 4.4	71.47 ± 0.9	14.08 ± 3.6	54.46 ± 0.6	18.75 ± 4.1	43.54 ± 3.4	30.95 ± 3.4	67.07 ± 0.9	15.34 ± 2.0
5	<50 (24.23 ± 1.4)	-	61.20 ± 1.7	16.81 ± 2.2	<50 (18.68 ± 1.9)	-	<50 (5.86 ± 0.5)	-	<50 (25.59 ± 1.9)	-
6	<50 (6.04 ± 2.8)	-	48.05 ± 0.9	24.60 ± 2.6	<50 (18.68 ± 1.9)	-	<50 (3.91 ± 0.3)	-	<50 (7.57 ± 0.5)	-
7	58.42 ± 4.6	24.58 ± 6.3	69.84 ± 1.1	13.42 ± 1.7	<50 (13.88 ± 5.1)	-	62.58 ± 0.7	19.18 ± 3.2	65.26 ± 0.2	17.55 ± 2.9
8	41.04 ± 1.2	28.86 ± 4.7	65.45 ± 1.9	15.68 ± 2.3	<50 (19.96 ± 2.7)	-	<50 (7.06 ± 2.4)	-	49.95 ± 1.6	27.21 ± 4.3
9	46.70 ± 2.8	22.16 ± 2.8	66.72 ± 1.7	15.21 ± 2.2	<50 (19.96 ± 2.7)	-	<50 (6.48 ± 2.2)	-	51.95 ± 0.8	24.60 ± 3.5
10	<50 (6.13 ± 0.4)	-	<50 (10.60 ± 10.7)	-	<50 (-2.88 ± 0.5)	-	<50 (2.35 ± 1.6)	-	<50 (0.85 ± 2.1)	-
11	NT	NT	NT	NT	NT	NT	NT	NT	NT	NT



12	<50 (6.36 ± 2.2)	-	<50 (29.66 ± 5.2)	-	<50 (10.04 ± 1.1)	-	<50 (6.41± 2.2)	-	<50 (8.36 ± 2.6)	-
Paclitaxe 1		13.17 ± 0.5		0.92 ± 3.3		0.011 ± 0.0005		0.0028 ± 0.00007		0.69 ± 0.13

<sup>a</sup> Sample tested in triplicate and in two separate experiments at **20 µg/mL**; <sup>b</sup> % Inhibition <50 deemed inactive; <sup>c</sup>  $IC_{50}$  ≥20 deemed inactive; NT = Not tested; Samples **1-4** stand for malabaricone A-D; Samples **5-9** stand for promalabaricone B, promalabaricone C, acyl phenol, ericanone and mono hydrated malabaricone C; Samples **10-14** stand for promalabaricane B, promalabaricane (without carbonyl group in adjoining nonane chain), dihydro-promalabaricane B, dihydro-promalabaricane C and carboxy malabaricone B.

**Table 2:  $^1\text{H}$  NMR ( $\text{CD}_3\text{OD}$ , 200 MHz) &  $^{13}\text{C}$  NMR ( $\text{CD}_3\text{OD}$ , 50 MHz) data for compounds 1-4.**

Position	1		2		3		4	
	$\delta_{\text{H}}(\text{J}_{\text{H-H}})$ Hz	$\delta_{\text{C}}$	$\delta_{\text{H}}(\text{J}_{\text{H-H}})$ Hz	$\delta_{\text{C}}$	$\delta_{\text{H}}(\text{J}_{\text{H-H}})$ Hz	$\delta_{\text{C}}$	$\delta_{\text{H}}(\text{J}_{\text{H-H}})$ Hz	$\delta_{\text{C}}$
1	-	209.61	-	209.64	-	209.63	-	209.59
2	2.97, t (7.6)	45.67	3.19, t (7.2)	45.69	2.95, t (7.2)	45.70	2.95, t (7.4)	45.79
3	1.56-1.53, m	36.60	1.57-1.50, m	32.67	1.57-1.50, m	32.85	1.49-1.46, m	32.88
4	1.48-1.46, m	32.63	1.20, s	30.45	1.21, s	30.57	1.40-1.46, m	30.65
5	1.19, s	30.44	1.20, s	30.26	1.21, s	30.26	1.14, s	30.27
6	1.19, s	25.66	1.20, s	25.66	1.21, s	25.69	1.14, s	25.64
7	1.48-1.46, m	30.25	1.20, s	30.26	1.21, s	30.49	1.14, s	30.53
8	1.56-1.53, m	36.60	1.50-1.42, m	30.26	1.45-1.41, m	30.57	1.49-1.46, m	30.65
9	2.44, t (7.0)	36.89	2.36, t (7.2)	36.89	2.32, t (7.8)	36.22	2.32, t (8.0)	36.66
10	-	126.51	-	126.53	-	135.74	-	137.81
11	7.19-6.94, m	129.32	6.84, dd (8.4, 2.2)	129.33	6.47, d (2.0)	116.45	6.48, d (2.0)	109.71
12	7.19-6.94, m	129.16	6.55, dd (8.2, 2.2)	129.18	-	145.86	-	148.91
13	7.19-6.94, m	143.91	-	143.92	-	143.90	-	146.75
14	7.19-6.94, m	129.16	6.55, dd (8.2, 2.2)	129.18	6.53, d (8.0)	116.13	6.53, d (8.0)	108.86
15	7.19- 6.94, m	129.32	6.84, dd (8.4, 2.2)	129.33	6.49, dd (8.0, 2.0)	120.61	6.47, dd (8.0, 2.0)	122.06
16	-	111.41	-	111.34	-	111.32	-	111.37
17	-	163.35	-	163.35	-	163.31	-	163.40
18	6.21, d (8.2)	108.83	6.19, d (8.2)	108.34	6.21, d (8.2)	108.30	6.20, d (8.2)	108.38
19	7.05, t (8.2)	136.74	7.06, t (8.2)	136.80	7.06, t (8.2)	136.78	7.03, t (8.2)	136.79
20	6.21, d (8.2)	108.33	6.23, d (8.2)	108.34	6.21, d (8.2)	108.30	6.20, d (8.2)	108.38
21	-	163.35	-	163.35	-	163.31	-	163.40
22	-	-	-	-	-	-	5.69, s	101.81

**Table 3:  $^1\text{H}$  NMR ( $\text{CD}_3\text{OD}$ , 200 MHz) &  $^{13}\text{C}$  NMR ( $\text{CD}_3\text{OD}$ , 50 MHz) data for compounds 5-9.**

Position	5		6		7		8		9	
	$\delta_{\text{H}}(\text{J in Hz})$	$\delta_{\text{C}}$	$\delta_{\text{H}}(\text{J in Hz})$	$\delta_{\text{C}}$	$\delta_{\text{H}}(\text{J in Hz})$	$\delta_{\text{C}}$	$\delta_{\text{H}}(\text{J in Hz})$	$\delta_{\text{C}}$	$\delta_{\text{H}}(\text{J in Hz})$	$\delta_{\text{C}}$
1	-	205.68	-	204.21	-	208.26	2.43, t (7.0)	31.27	-	209.64
2	2.97, t (7.0)	47.58	2.91, t (7.4)	34.59	3.13, t (7.0)	44.79	1.55, m	28.85	2.95, t (7.2)	45.70
3	1.61-1.51, m	40.57	1.60-1.53, m	31.29	1.67-1.66, m	31.90	4.16, m	62.07	1.57-1.50, m	32.81
4	1.21, s	35.56	1.22, s	28.68	1.16, brs	29.64	2.91, t (7.50)	34.32	1.21, s	30.57
5	1.21, s	35.40	1.22, s	24.33	1.16, brs	29.54	-	204.23	1.21, s	30.22
6	1.21, s	33.57	1.22, s	28.68	1.16, brs	29.54	2.91, t (7.50)	31.27	1.21, s	25.65
7	1.21, s	35.56	1.22, s	28.86	1.16, brs	29.40	4.16, m	62.07	1.21, s	30.46
8	1.61-	40.57	1.60-	28.86	1.16, brs	29.34	1.55, m	28.77	1.45-	30.56

	1.51, m		1.53, m						1.41, m	
9	2.49, t (7.0)	42.13	2.39, t (7.0)	34.37	1.16, brs	29.34	2.43, t (7.0)	31.27	2.32, t (7.8)	36.19
10	-	137.70	-	132.41	1.16, brs	29.34	-	132.49	-	135.75
11	7.00, dd (8.4, 2.8)	127.55	6.52, d (2.0)	115.67	1.16, brs	29.34	6.94, d (8.5)	118.87	6.47, d (2.0)	116.45
12	6.72, dd (8.4, 2.8)	113.60	-	144.95	1.16, brs	24.48	6.64, d (8.5)	115.04	-	145.80
13	-	156.08	-	143.05	1.16, brs	22.66	-	155.16	-	143.84
14	7.00, dd (8.4, 2.8)	111.60	6.59, d (8.2)	115.41	0.83, t (6.0)	14.08	6.94, d (8.5)	115.04	6.53, d (8.0)	116.13
15	6.72, dd (8.4, 2.8)	129.95	6.37, dd (8.2, 2.0)	129.06	-	110.09	6.64, d (8.5)	112.75	6.49, dd (8.0, 2.0)	120.62
16	-	113.77	-	115.00	-	161.19	-	112.75	-	111.29
17	-	193.67	-	155.21	6.39, d (8.2)	108.42	6.94, d (8.5)	132.46	-	163.31
18	3.08, dd (18.0, 3.6) 2.76, dd (18.0, 3.6)	42.13	3.04, dd (18.2, 3.6) 2.78, dd (18.2, 3.6)	28.86	7.21, t (8.2)	135.73	6.64, d (8.5)	118.87	6.21, d (8.2)	108.29
19	4.38, m	63.62	-	62.09	6.39, d (8.2)	108.42	-	155.16	7.06, t (8.2)	136.78
20	2.67, dd (17.8, 5.0) 2.75, dd (17.8, 5.0)	40.57	2.66, dd (18.2, 7.4) 2.75, dd (18.2, 7.4)	34.59	-	161.19	6.64, d (8.5)	118.87	6.21, d (8.2)	108.30
21	-	198.05	-	204.21	-	-	6.94, d (8.5)	107.18	-	163.26

Table 4:  $^1\text{H}$  NMR ( $\text{CD}_3\text{OD}$ , 200 MHz) &  $^{13}\text{C}$  NMR ( $\text{CD}_3\text{OD}$ , 50 MHz) data for compounds 10-12.

Position	10		11		12	
	$\delta_{\text{H}}$ (J in Hz)	$\delta_{\text{C}}$	$\delta_{\text{H}}$ (J in Hz)	$\delta_{\text{C}}$	$\delta_{\text{H}}$ (J in Hz)	$\delta_{\text{C}}$
1	3.08-3.04, m	36.04	3.09-2.97, m	204.21	-	209.63
2	1.33, s	30.44	1.33, s	34.59	3.15, t (7.2)	45.70
3	1.66-1.56, m	40.57	1.60-1.54, m	31.29	1.72-1.65, m	32.85
4	1.33, s	30.44	1.31, s	28.68	1.33, s	30.57
5	1.33, s	30.21	1.31, s	24.33	1.33, s	30.26
6	1.33, s	30.21	1.31, s	28.68	1.33, s	25.69
7	1.33, s	30.21	1.31, s	28.86	1.33, s	30.49
8	1.66-1.54, m	30.44	1.60-1.54, m	28.86	1.65-1.54, m	30.57
9	2.54, t (7.0)	42.13	2.24, t (7.0)	34.37	2.51, t, (7.8)	36.22
10	-	134.88	-	132.41	-	135.74
11	6.68, dd (8.4, 2.8)	127.55	6.52, d (2.0)	115.67	6.50, dd (2.0, 8.0)	116.45
12	6.97, dd (8.4, 2.8)	113.60	-	144.95	7.00, d (8.0)	116.13
13	-	156.21	-	143.05	-	143.90
14	6.97, dd (8.4, 2.8)	108.34	6.72, d (8.2)	115.41	-	145.86
15	6.68, dd (8.4, 2.8)	130.23	6.51, dd (8.2, 2.0)	129.06	6.73, d (2.0)	120.61
16	-	115.98	-	115.00	-	111.32
17	-	193.67	-	155.21	-	163.31
18	3.32-3.31, m	36.04	3.32-3.31, m	28.86	6.41, d (8.2)	108.30

			3.08-3.04, m			
19	4.30, m,	64.07	4.48, m	62.09	7.24, t (8.2)	136.78
20	3.15-3.11, m	33.00	3.15-3.11, m, 3.08-3.04, m	34.59	6.41, d (8.2)	108.30
21	-	198.05	-	204.21	-	163.31

### Supplementary information

Supplementary Information is available for this paper.

**Annexure 1:** Supporting Information (Spectroscopic data consisting IR, UV,  $^1\text{H}$  NMR,  $^{13}\text{C}$  NMR, DEFT, HMBC, EIMS, HRESI-MS of compounds (1-9), X-ray diffraction of compounds) were enclosed in attached file. Crystallographic data for the structures reported in this paper have been deposited with the Cambridge Crystallographic Data Centre (CCDC). Copies of the data can be obtained, free of charge, on application to Director, CCDC, 12 Union Road, Cambridge CB2, 1EZ, UK (fax: + 44-(0)1223-336033 or email: deposit@ccdc.cam.ac.uk

### ACKNOWLEDGEMENTS

We express our sincere gratitude to Dr. David G. I. Kingston, Department of Chemistry, Virginia Tech, Blacksburg, Virginia 24061, USA for fostering to collaborate with Prof. Esperanza J. Carcache de Blanco, College of Pharmacy, The Ohio State University, Ohio, Columbus, USA. We acknowledge Dr. Dmitriy Uchenik, Dr. Deepa Krishnan, OSU College of Pharmacy instrumentation facility, for allowing acquisition of MS

data and Mrs. Mamata V. Joshi for her excellent effort to acquire 2D-NMR data by using National Instrumental Facility, Tata Institute of Fundamental Research (TIFR) Centre, Colaba, Mumbai. Authors are very much grateful to Head of Division, Bio-Organic Division and Group Director of Bio-science Group for their continuous encouragement and ethical support.

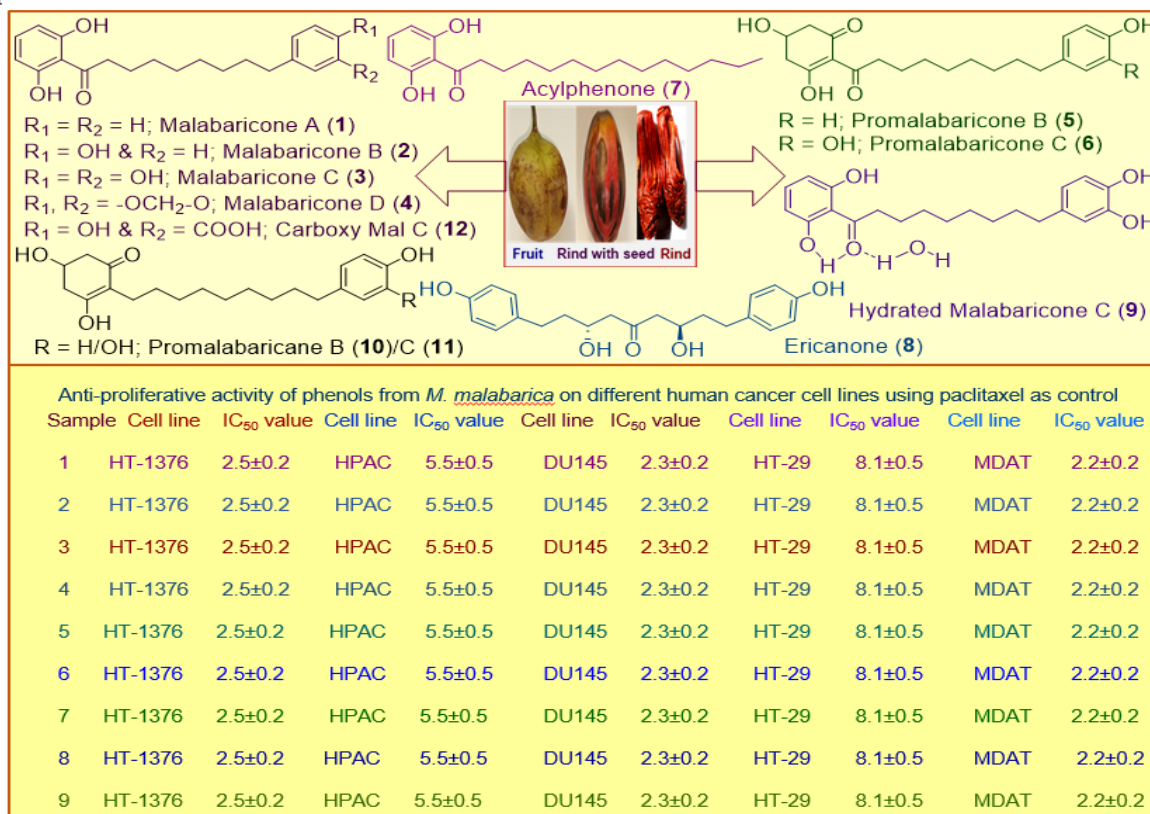
### Author contribution statement

AKB performed isolation, structural characterization, chemical transformation/reaction and drafted manuscript. IC and ESA contributed to the samples/reagents/materials/analysis tools and analysed anti-proliferative assay data. SF contributed analysis tools and analyzed the XRD data of crystals, structure analysis and computation. EJCB supervised biological experimental, analysed anti-proliferative assay data, reviewed the manuscript, and manage acquiring HRESI-MS and LR ESI-MS data.

### Conflict of interest

The authors declare that there is no conflict of interest regarding the publication of this article.

### Graphicalabstract



## REFERENCES

1. T. J. Zachariah, N. K. Leela, K. M. Maya, J. Rema, P. A. Mathew, T. M. Vipin and B. Krisnsmoorthy. Chemical composition of leaf oils of *Myristica beddomei*, *Myristica fragrans* (Houtt) and *Myristica malabarica* (Lamk). *J. Spices and Aromatic Crops*, 2008; 17: 10-15.
2. B. N. Sastri. *The Wealth of India. Raw Materials*. Council of Scientific and Industrial Research: New Delhi, 1962; 6: 479-487.
3. P. K. Chelladurai, R. Ramalingam. *Myristica malabarica*: A comprehensive review. *J. Pharmacogn. Phytochem*, 2017; 6: 255-258.
4. The Plant List. A working list of plant species. Royal Botanic Gardens, Kew and Missouri Botanical Garden (Accessed January 18, 2019). <http://www.theplantlist.org/tpl1.1/search?q=Myristica>
5. B. Krishnamoorthy, J. Rema. Nutmeg and Mace. In *Handbook of Herbs and Spices*. Peter, K. V., Ed. Woodhead Publishing Ltd.: Cambridge, UK, 2001; 238-248.
6. K. K. Purushothaman, A. Sarada, J. D. Connolly. Structure of malabaricanol - a lignan from the aril of *Myristica malabarica* Lam. *Ind. J. Chem*, 1974; 23B: 46-48.
7. K. K. Purushothaman, A. Sarada, J. D. Connolly. Malabaricones A-D, novel diarylnonoids from *Myristica malabarica* Lam (Myristicaceae). *J. Chem. Soc., Perkin Trans*, 1977; 1: 587-588.
8. F. Filleur, C. Pouget, D. P. Allais, M. Kaouadji, A. J. Chulia. Lignans and neolignans from *Myristica argentea* Warb. *Nat. Prod. Lett*, 2002; 16: 1-7.
9. P. T. Thuong, T. M. Hung, N. M. Khoi, H. T. Nhung, N. T. Chinh, N. T. Quy, T. S. Jang, M. Na. Cytotoxic and anti-tumor activities of lignans from the seeds of Vietnamese nutmeg *Myristica fragrans*. *Arch. Pharm. Res*, 2014; 37: 399-403.
10. C. Y. Ragasa, O. B. Torres, J. V. V. Tongco, R. A. Razal, C.-C. Shen. Resorcinols from *Myristica philippensis* Lam. *J. Chem. Pharm. Res*, 2013; 5: 614-616.
11. M. Hattori, X. W. Yang, Y. Z. Shu, N. Kakiuchi, Y. Tezuka, T. Kikuchi, T. Namba. New constituents of the aril of *Myristica fragrans*. *Chem. Pharm. Bull*, 1988; 36: 648-653.
12. X. W. Yang, X. Huang, M. Ahmat. New neolignan from seed of *Myristica fragrans*. *China J. Chin. Mater. Med*, 2008; 33: 397-402.
13. X. W. Yang, X. Huang, L. Ma, Q. Wu, W. Xu. The Intestinal Permeability of Neolignans from the Seeds of *Myristica fragrans* in the Caco-2 Cell Monolayer Model. *Planta Med.*, 2010; 76: 1587-1591.
14. A. C. Talukdar, N. Jain, S. De, H. G. Krishnamurty. An isoflavone from *Myristica malabarica*. *Phytochemistry*, 2000; 53: 155-157.
15. F. M. Dean. *Naturally Occurring Oxygen Ring Compounds*, Butterworths: London, UK, 1963; 288-289.
16. K. D. Arunachalam, Subhasini. Preliminary phytochemical investigation and wound healing activity of *Myristica andamanica* leaves in Swiss albino mice. *Journal of Medicinal Plants Research*, 2011; 5: 1095-1106.
17. T. J. Mabry, K. R. Markham, M. B. Thomas. *The Systematic Identification of Flavonoids*, Springer-Verlag: New York, 1970; 36-38.
18. T. D. Cuong, C. J. Lim, T. Trang, Y. H. Bae. Compounds from the seed of *Myristica fragrans* and their cytotoxic activity. *Nat. Prod. Sci*, 2012; 18: 97-101.
19. A. Manna, S., DeSarkar, S. De, A. K. Bauri, S. Chattopadhyay, M. Chatterjee. Impact of MARK and P13K/AKT signalling pathways on Malabaricone-A induced cytotoxicity in U937, a histiocytic lymphoma cell line. *Int. Immunopharmacol*, 2016; 39: 34-40.
20. A. Manna, S. DeSarkar, S. De, A. K. Bauri, S. Chattopadhyay, M. Chatterjee. The variable chemotherapeutic response of Malabaricone-A in leukemic and solid tumor cell lines depends on the degree of redox imbalance. *Phytomedicine*, 2015; 22: 713-723.
21. A. Manna, P. Saha, A. Sarkar, D. Mukhopadhyay, A. K. Bauri, D. Kumar, P. Das, S. Chattopadhyay, M. Chatterjee. Malabaricone-A Induces A redox Imbalance That Mediates Apoptosis in U937 Cell Line. *PLOS ONE*, 2012; 7: e36938.
22. M. Tyagi, A. K. Bauri, B. S. Patro, S. Chattopadhyay. Mechanism of the malabaricone-C induced toxicity to the MCF cell line. *Free Rad. Res*, 2014; 48: 446-477.
23. M. Tyagi, B. Maity, B. Saha, A. K. Bauri, M. Subramaniam, S. Chattopadhyay, B. Patro. The spice derived phenolic, malabaricone B induces mitochondrial damage in lung cancer (A549) cells via p53-independent pathway. *Food & Function*, 2018; 14, 9(11): 5715-5727.
24. M. Tyagi, R. Bhattacharyya, A. K. Bauri, B. S. Patro, S. Chattopadhyay. DNA damage dependent activation of checkpoint kinase-1 and mitogen activated protein kinase p38 are required in malabaricone-C induced mitochondrial cell death. *Biochim. Biophys. Acta*, 2014; 1840: 1014-1027.
25. M. Tyagi, A. K. Bauri, S. Chattopadhyay, B. S. Patro. Thiol anti-oxidants sensitize Malabaricone C induce cancer cell death via reprogramming redox p53 and NF-kB proteins *in vitro* and *vivo*. *Free Rad. Biol. Med*, 2020; 148: 182-199.
26. B. S. Patro, M. Tyagi, S. Chattopadhyay. Comparative nuclease and anti-cancer properties of naturally occurring malabaricones. *Bioorg. & Med. Chem*, 2010; 7043-7051.
27. B. S. Patro, A. K. Bauri, S. Mishra, S. Chattopadhyay. Anti-oxidant activity of *M. malabarica* Extracts and their constituents. *Agri. & Food Chem*, 2005; 53: 6912-6918.



28. W. J. J. O. de Wilde. Synonymic Checklists of the Vascular Plants of the World. *Blumea*, 1997; 42: 148.
29. V. C. Pham, A. Jossang, T. Sévenet, B. Bodo. Cytotoxic acylphenols from *Myristica maingayi*. *Tetrahedron*, 2000; 56: 1707-1713.
30. S. A. Muchtaridi, A. Apriyantono, R. Mustarichie. Identification of compounds in the essential oil of nutmeg seeds (*Myristica fragrans* Houtt.) that inhibit locomotor activity in mice. *Int. J. Mole. Sci.*, 2010; 11: 4771-4781.
31. G. Singh, P. Marimuthu, C. S. De Heluani, C. Catalan. Anti-microbial and anti-oxidant potentials of essential oil and acetone extract of *Myristica fragrans* Houtt. (Aril Part). *J. Food Sci.*, 2005; 70: 141-148.
32. S. Cao, J. K. Schilling, J. S. Miller, A. Randrianasolo, R. Andriantsiferana, V. E. Rasamison, D. G. I. Kingston. New Cytotoxic Alkyl Phloroglucinols from *Protorhus thouvenotii*. *Planta Med.*, 2004; 70: 683-684.
33. A. K. Bauri, Y. Du, P. J. Brodie, S. Foro, D. G. I. Kingston. Anti-proliferative Acyl Phenol and Arylnonanoids from the Fruit Rind of *Myristica malabarica*. *Chemistry & Biodiversity*, 2022; e202200343.
34. R. Barman, P. K. Bora, J. Saikia, P. Kemprai, S. P. Saikia, S. Haldar, D. Banik. Nutmegs and wild nutmegs: An update on ethnomedicines, phytochemicals, pharmacology, and toxicity of the Myristicaceae species. *Phytother. Res.*, 2021; 1-28.
35. T. K. Lim. Edible Medicinal And Non Medicinal Plant, 2011; 3: 572-574.
36. M. A. Othamana, Y. Sivasothy, Y. C. Looi, A. Ablatc, J. Mohamad, M. Litaudond, K. Awanga, *Fitoterapia*, 2016; 111: 12-14.
37. S. Krishna, H. Somanathan. Secondary removal of *Myristica Fauta* (*Myristicaceae*) seeds by crabs in *Myristica swamp* forest in India. *J. Trop. Ecol.*, 2014; 30: 259-263.
38. M. D. S. Chandran, D. K. Mesta. *Myristica Swamps*: Remnants of Primeval Tropical Forests of Western Ghats Sahyadri. Western Ghats Biodiversity Information system SAHYADRI E-NEWS: Issue XIII, 1997.
39. W. J. J. O. de Wilde. Flora Malesiana Series 1. Nationaal Herbarium Nederiand, Universiteit Leiden branch, 2000.
40. S. Hada, M. Hattori, X. W. Yang, Y. Z. Shu, N. Kakiuchi, Y. Tezuka, T. Kikuchi, T. Namba. New neolignans of the aril of *Myristica fragrans*. *Phytochemistry*, 1988; 27: 563-568.
41. P. T. Thuong, T. M. Hung, N. M. Khoi, H. T. M. Nhung, N. T. Chinh, N. T. Quy, M. Na. Cytotoxic and anti-tumor activities of lignans from the seeds of Vietnamese nutmeg *Myristica fragrans*. *Arch. Pharmacol. Res.*, 2014; 37: 399-403.
42. B. Nagaraju, S. H. Sahar, B. Ali, K. Z. Neha, A. Zahra, C. Zothanmawia, A. Surendranatha. Anxiolytic effect of *Myristica fragrans*. *Int. J. Phytother Res.*, 2013; 3: 1-7.
43. P. Chumkaew, T. Srisawat. New neolignans from the seeds of *Myristica fragrans* and their cytotoxic activities. *Journal of Natural Medicines*, 2018; 73: 273-277.
44. M. A. Saputro, N. Andarwulan, D. N. Faridah. Physical characterization and essential oil properties of West Sumatra mace and nutmeg seed (*Myristica fragrans* Houtt) at different ages at harvest. *J. Pharmacogn. Phytochem.*, 2016; 5: 371-37.
45. V. M. M. Valente, G. N. Jham, O. D. Dhingra, I. Ghiviriga. Composition and anti-fungal activity of the Brazilian *Myristica fragrans* Houtt. essential oil. *J. Food Saf.*, 2011; 31: 197-202.
46. M. T. Ha, N. K. Vu, T. H. Tran, J. H. Kim, M. H. Woo. Phyto chemical and pharmacological properties of *Myristica fragrans* Houtt.: an updated review. *Arch. Pharm. Res.*, 2020; 43: 1067-1092.
47. Y. M. Chong, W. F. Yin, C. Y. Ho, M. R. Mustafa, A. Hamid, A. Hadi, K. Awang, P. Narrima, C-L. Koh, D. R. Appleton, K-G. Chan. Malabaricone C from *Myristica cinnamomea* exhibits anti-quorum sensing activity. *J. Nat. Prod.*, 2011; 74: 2261-6224.
48. N. F. Cooray, E. R. Jansz, S. Wimelesana, T. P. Wijesekera, B. M. Nair. Acylresorcinols from Seed Kernels of *Myristica dactyloides*. *Phytochemistry*, 1987; 26: 3369-3371.
49. S. Subha, B. Vijayakumar, K. Prudhviraj, M. V. Anandhi, M. Shankar, M. Nishanthi. Pharmacognostic and preliminary phytochemical investigation on leaf extracts of *Myristica dactyloides* Gaertn. *Int. J. Phytopharm.*, 2013; 4: 18-23.
50. B. Vidhya, P. T. Venkatesh, A. Vishnubharath, M. Tejaashwine, P. Eganathan, J. Saranya, P. Sujanalpal. Essential oil composition, anti-oxidant and nutritional properties of fruit pericarp of *Myristica beddomei* King ssp. *ustulata* de Wilde-an endangered tree species. *Anal. Chem. Lett.*, 2015; 5: 21-30.
51. S. Fajriah, A. Darmawan, H. S. Megawati, S. Kosela, M. Hanafi. New cytotoxic compounds from *Myristica fatua* Houtt. leaves against MCF-7 cell lines. *Phytochem. Lett.*, 2017; 20: 36-39.
52. S. M. A. Wahab, Y. Sivasothy, S. Y. Liew, M. Litaudon, J. Mohamad, K. Awang. Natural cholinesterase inhibitors from *Myristica cinnamomea* King. *Bioorg. & Med. Chem. Lett.*, 2016; 26: 3785-3792.
53. C. Y. Ragasa, O. B. Torres, J. V. V. Tongco, R. A. Razal, C.-C. Shen. Resorcinols from *Myristica philippensis* Lam. *J. Chem. Pharm. Res.*, 2013; 5: 614-616.
54. B. Benni, A. J. Chulia, M. Kaouadji, P. Fondaneche. Diaryl nonanoids and their glycosides from *Erica cinerea*. *Tetra. Letts.*, 2011; 52: 1597-1600.
55. A. Agriga, M. Siwela. Monodora *Myristica* (Gaertn. Dunal: A Plant with Multiple Food, Health

- and Medicinal Applications: A Review. *Am. J. Food Tech*, 2017; 12: 271-184.
56. E. Soepadmo, L. G. Saw, R. C. K. Chung. Tree Flora of Sabah and Sarawak. Forest Research Institute Malaysia; Kuala Lumpur, 2002; 1-6.
57. M. J. T. G. Gonzalez, M. M. M. Pinto, A. Kijjoa, C. Anantachoke, W. Herz. Stilbenes and Other Constituents of *Knema austrosiamensis*. *Phytochemistry*, 1993; 32: 433-438.
58. T. H. Giap, P. M. Duc, N. V. The, M. Popava, V. Bankova, C. T. Hue, V. T. K. Oanh, N. T. M. Hang, H. N. Van, T. N. Le. Chemical constituents and biological activities of the fruits of *Knema Pachycarpa* de Wilde. *Nat. Prodt. Res*, 2019; 35: 455-464.
59. V. Vichai, K. Kirtikara. Sulforhodamin B colourimetric assay for cytotoxicity screening. *Nat. Protoc*, 2006; 1: 1112-1116.
60. G. D. Anaya-Eugenio, E. M. Addo, N. Ezzone, M. Henkin, T. N. Ninh, Y. Ren, D. D. Soejarto, A. D. Kinghorn, E. de Blanco Carcache. Caspase-dependent apoptosis in prostate cancer cells and zebrafish by corchorusoside C from *Streptocaulon juvenas*. *J. Nat. Prod*, 2019; 82: 1645-1655.

**Annexure 1: Supplementary information contents.**

Entry No.	Legendary title
Figure S1	<sup>1</sup> H NMR spectrum (CD <sub>3</sub> OD, 200 MHz) of compound <b>1</b> (Malabaricone A)
Figure S2	<sup>13</sup> C NMR spectrum (CD <sub>3</sub> OD, 50 MHz) of compound <b>1</b> (Malabaricone A)
Figure S3	HR-ESI (negative mode) mass spectrum of compound <b>1</b> (Malabaricone A)
Figure S4	ORTEP diagram and crystal data of compound <b>1</b> (Malabaricone A)
Figure S5	<sup>1</sup> H NMR spectrum (CD <sub>3</sub> OD, 200 MHz) of compound <b>2</b> (Malabaricone B)
Figure S6	<sup>13</sup> C NMR spectrum (CD <sub>3</sub> OD, 50 MHz) of compound <b>2</b> (Malabaricone B)
Figure S7	HR-ESI (positive mode) mass spectrum of compound <b>2</b> (Malabaricone B)
Figure S8	ORTEP diagram of compound <b>2</b> crystallized as twin molecules (Malabaricone B)
Figure S9	<sup>1</sup> H NMR spectrum (CD <sub>3</sub> OD, 200 MHz) of compound <b>3</b> (Malabaricone C)
Figure S10	<sup>13</sup> C NMR spectrum (CD <sub>3</sub> OD, 50 MHz) of compound <b>3</b> (Malabaricone C)
Figure S11	HRESI-MS (positive mode) spectrum of compound <b>3</b> (Malabaricone C)
Figure S12	ORTEP diagram and crystal data of compound <b>3</b> (Malabaricone C)
Figure S13	<sup>1</sup> H NMR (CDCl <sub>3</sub> , 200 MHz) spectrum of compound <b>4</b> (Malabaricone D)
Figure S14	<sup>13</sup> C NMR spectrum of compound <b>4</b> (Malabaricone D)
Figure S15	HRESI-MS of compound <b>4</b> (Malabaricone D)
Figure S16	ORTEP diagram and crystal data of compound <b>4</b> (Malabaricone D)
Figure S17	<sup>1</sup> H NMR (CD <sub>3</sub> COCD <sub>3</sub> , 200 MHz) spectrum of compound <b>5</b> (Promalabarinone B)
Figure S18	<sup>1</sup> H NMR spectrum of compound <b>5</b> (Promalabarinone B), VT, USA
Figure S19	<sup>13</sup> C NMR (CD <sub>3</sub> COCD <sub>3</sub> , 50 MHz) spectrum of compound <b>5</b> (Promalabarinone B)
Figure S20	HRESI-MS of compound <b>5</b> (Promalabarinone B)
Figure S21	HRESI-MS of compound <b>5</b> (Promalabarinone B)
Figure S22	ORTEP diagram and crystal data of compound <b>5</b> (Promalabarinone B)
Figure S23	<sup>1</sup> H NMR (CD <sub>3</sub> OD, 200 MHz) spectrum of compound <b>6</b> (Promalabarinone C)
Figure S24	<sup>1</sup> H NMR (CD <sub>3</sub> OD, 200 MHz) spectrum of compound <b>6</b> with expansion
Figure S25	<sup>13</sup> C NMR (CD <sub>3</sub> OD, 50 MHz) spectrum of compound <b>6</b> (Promalabarinone C)
Figure S26	HRESI-MS of compound <b>6</b> (Promalabarinone C)
Figure S27	<sup>1</sup> H NMR (CD <sub>3</sub> OD, 200 MHz) spectrum of compound <b>7</b> (Acyl phenol)
Figure S28	Expansion of <sup>1</sup> H NMR spectrum of compound <b>7</b> (Acyl phenol)
Figure S29	<sup>13</sup> C NMR spectrum of compound <b>7</b> (Acyl phenol)
Figure S30	HRESI-MS (negative mode) of compound <b>7</b> (Acyl phenol)
Figure S31	ORTEP diagram and crystal data of compound <b>7</b> (recorded from TU, Germany)
Figure S32	<sup>1</sup> H NMR (CD <sub>3</sub> OD, 200 MHz) spectrum of crude product yielded on treatment with H <sub>2</sub> SO <sub>4</sub> (dehydration reaction: promalabarinone B treated with concentrated H <sub>2</sub> SO <sub>4</sub> produced malabaricone B)
Figure S33	Expansion of <sup>1</sup> H NMR (CD <sub>3</sub> OD, 200 MHz) spectrum of crude product yielded on treatment with H <sub>2</sub> SO <sub>4</sub> (dehydration reaction: promalabarinone B treated with concentrated H <sub>2</sub> SO <sub>4</sub> produced malabaricone B)
Figure S34	HR-ESIMS [MH <sup>+</sup> = 343.1905 Da] of the product obtained from by chemical transformation with acid
Figure S35	HRESI-MS spectrum [MH <sup>+</sup> = 343.1905Da] of product yielded by chemical transformation of compound <b>5</b> (Promalabarinone B) to <b>2</b> (malabaricone B) on treatment with H <sub>2</sub> SO <sub>4</sub> in MeOH by stirring by 12h)
Figure S36	HRESI-MS spectrum [MH <sup>+</sup> = 359.1853 Da & [MH <sup>+</sup> ]: 376.095 Da] of product afforded by chemical transformation of compound <b>6</b> by H <sub>2</sub> SO <sub>4</sub> treatment and ESIMS spectrum of respective product recorded from VT, USA
Figure S37	HRESI-MS spectrum of compound <b>6</b> (promal-C, in positive mode), recorded from OSU, USA
Figure S38	<sup>1</sup> H NMR (CDCl <sub>3</sub> , 500 MHz) spectrum of compound <b>8</b>
Figure S39	<sup>1</sup> H NMR (CDCl <sub>3</sub> , 200 MHz) spectrum of crude compound <b>8</b>
Figure S40	<sup>13</sup> C NMR spectrum (CDCl <sub>3</sub> , 125 MHz) of compound <b>8</b>
Figure S41	HRESI-MS (positive mode) spectrum of compound <b>8</b> (Ericanone)
Figure S42	<sup>1</sup> H NMR spectrum (CD <sub>3</sub> COCD <sub>3</sub> , 200 MHz) of compound <b>9</b> (Hydrated malabaricone C)
Figure S43	Expansion of <sup>1</sup> H NMR spectrum (CD <sub>3</sub> COCD <sub>3</sub> , 200 MHz) of compound <b>9</b> (Hydrated malabaricone C)
Figure S44	<sup>13</sup> C NMR (CD <sub>3</sub> COCD <sub>3</sub> , 50 MHz) spectrum of compound <b>9</b> (Hydrated malabaricone C)
Figure S45	HRESI-MS (positive mode) spectrum of compound <b>9</b> (Hydrated malabaricone C)
Figure S46	ORTEP diagram and crystal data of compound <b>9</b> (Hydrated malabaricone C)
Figure S47	<sup>1</sup> H NMR spectrum (CD <sub>3</sub> OD, 200 MHz) of compound <b>10</b> (Promalabaricane B. No carbonyl group in aliphatic chain)
Figure S48	Expansion of <sup>1</sup> H NMR spectrum (CD <sub>3</sub> OD, 200 MHz) of compound <b>10</b> (Promalabaricane B. No

	carbonyl group in aliphatic chain)
Figure S49	$^{13}\text{C}$ NMR spectrum ( $\text{CD}_3\text{OD}$ , 50 MHz) of compound <b>10</b> (Promalabaricane B; No carbonyl group in aliphatic chain)
Figure S50	HRESI-MS (positive mode) of compound <b>10</b> (Promalabaricane B)
Figure S51	$^1\text{H}$ NMR spectrum ( $\text{CD}_3\text{COCD}_3$ , 200 MHz) of compound <b>11</b> (Promalabaricane C. No carbonyl group in aliphatic chain)
Figure S52	$^{13}\text{C}$ NMR spectrum ( $\text{CD}_3\text{COCD}_3$ , 50 MHz) of compound <b>11</b> (Promalabaricane C)
Figure S53	LRESI-MS (positive mode) of compound <b>11</b> (Promalabaricane C; No carbonyl group in aliphatic chain)
Figure S54	$^1\text{H}$ NMR ( $\text{CD}_3\text{COCD}_3$ , 200 MHz) of compound <b>12</b> (enrich aglycone yielded on acid hydrolysis glycoside)
Figure S55	$^{13}\text{C}$ NMR ( $\text{CD}_3\text{COCD}_3$ , 125 MHz) spectrum of compound <b>12</b> (enrich aglycone yielded on acid hydrolysis of glycoside)
Figure S56	$^1\text{H}$ NMR spectrum ( $\text{CD}_3\text{COCD}_3$ , 200 MHz) of aglycone yielded on acid hydrolysis of glycoside, a black mug hygroscopic in nature
Figure S57	Difference between malabaricone C & hydrated malabaricone C in $^1\text{H}$ NMR spectra
Figure S59	Graphical abstract
Chart C1	Flow diagram for isolation of secondary metabolites from defatted MeOH extract of dried rind of <i>M. malabarica</i>
Scheme 1	Scheme for acid hydrolysis of glycoside
Scheme 2	Scheme for acid hydrolysis of glycoside & separation of acid from phenol on treatment with $\text{NaHCO}_3$ solution

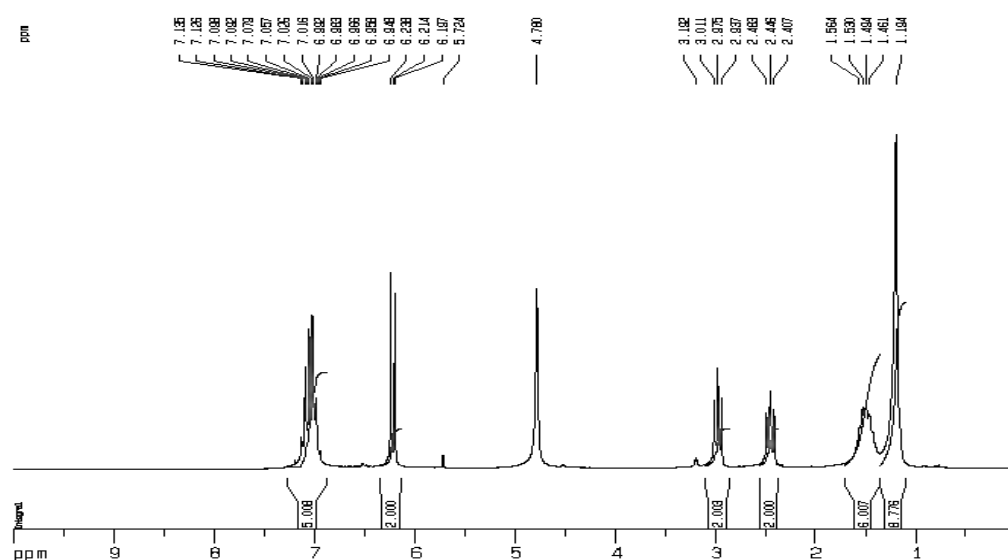


Figure S1:  $^1\text{H}$  NMR ( $\text{CD}_3\text{OD}$ , 200 MHz) spectrum of compound **1** (Malabaricone A).



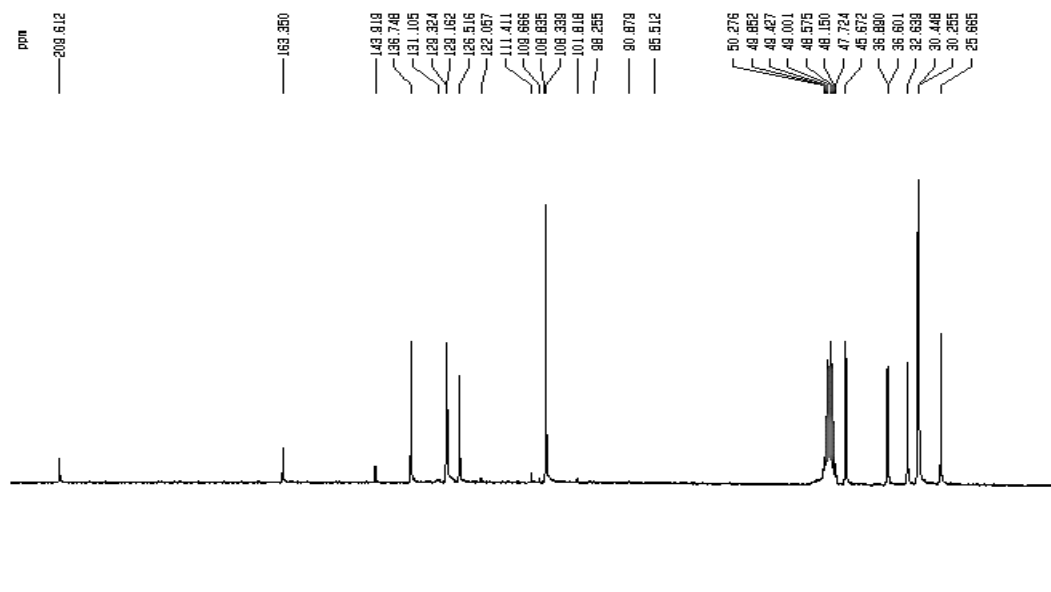


Figure S2:  $^{13}\text{C}$  NMR ( $\text{CD}_3\text{OD}$ , 50 MHz) spectrum of compound 1 (Malabaricone A).

MMA (Sample 7)

[ ] = 100  $\mu\text{g/mL}$

MODE: High Res - ESI (Negative)

T: FTMS - c ESI Full ms [200.0000-1500.0000]

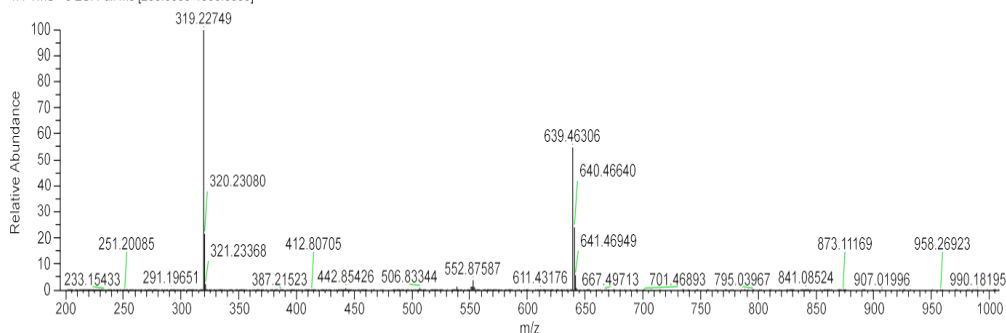


Figure S3: HRESI-MS spectrum of compound 1 (Malabaricone A).

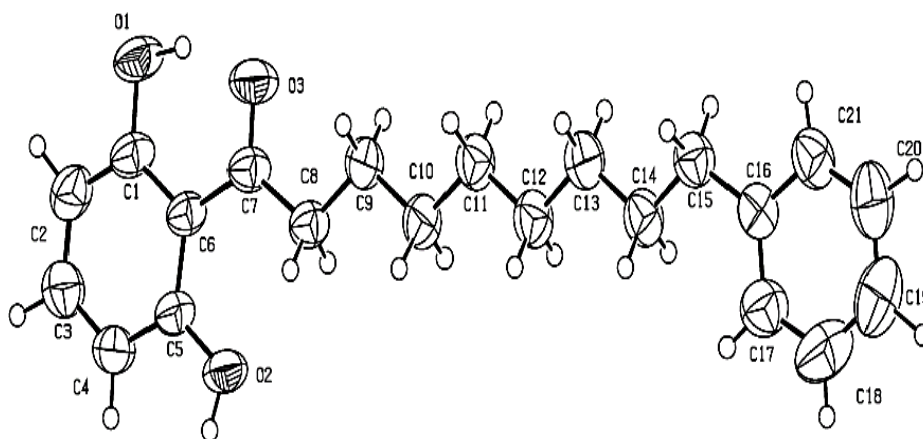
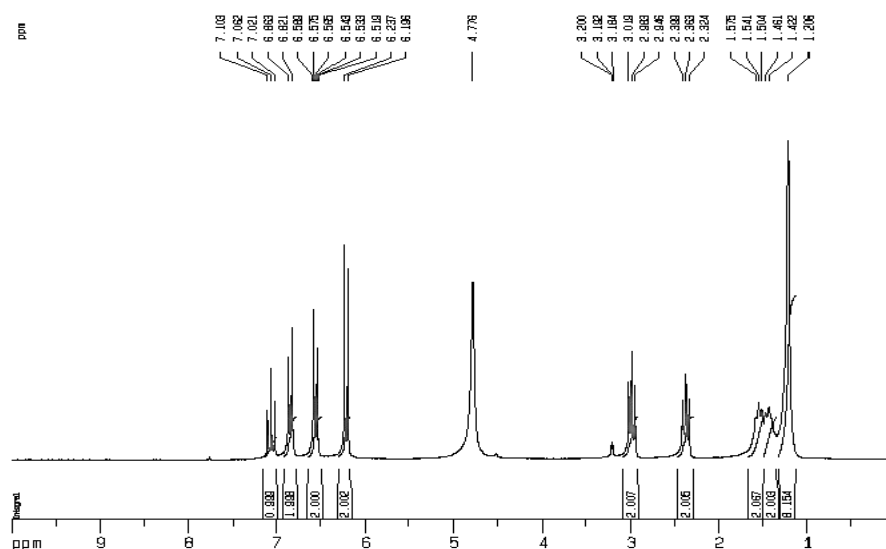


Figure S4: ORTEP diagram of compound 1 (Malabaricone A).

X-ray crystallographic analysis of compound **1** (Malabaricone A): Crystals of compound **1** were obtained from a mixture of ethyl acetate and hexane.

**Crystal data of compound 1** (Malabaricone A): monoclinic crystal (0.65 x 0.18 x 0.10) mm; space group name P2<sub>1</sub>/n. Unit cell dimension: a = 4.1831 (6) Å,  $\alpha$  = 90.00°; b = 32.562 (2) Å;  $\beta$  = 98.430 (10) °; c = 13.6270 (10) Å;  $\gamma$  = 90.00°; cell volume, V 1836.1(3); unit cell formula, Z = 4; crystal density diffraction,  $d_x$  = 1.181 Mg m<sup>-3</sup>. Number of independent reflections were measured 6403, number of independent reflections 3251 and number of independent reflections were observed [R (int.) = 0.044]

2092. Completeness of  $\theta$  was 67.09, 100%;  $\theta$  range for data collection 8.2 to 23.9°. Absorption correction: semi-empirical from equivalent. The structure was solved by direct methods and refined by a full matrix least squares on  $F^2$ . Final R indexes [ $R^2 > 2\sigma(F^2)$ ]:  $R1 = 0.046$ ,  $wR2 = 0.143$ ,  $S = 1.04$ . Absorption coefficient,  $\mu = 0.61 \text{ mm}^{-1}$ . Cell measured angle  $\theta_{\min}$  2.17 and  $\theta_{\max}$  67.09. Crystal description prism; crystal colour yellow. Diffraction temperature recorded 299 (2) K, diffraction radiation used monochromator graphite. Extinction correction was done SHELXL97; extinction coefficient 0.0029 (5). Large difference peak and hole = 0.22 and -0.14 e.Å<sup>-3</sup>.



**Figure S5:  $^1\text{H}$  NMR ( $\text{CD}_3\text{OD}$ , 200 MHz) spectrum of compound 2 (Malabaricone B).**

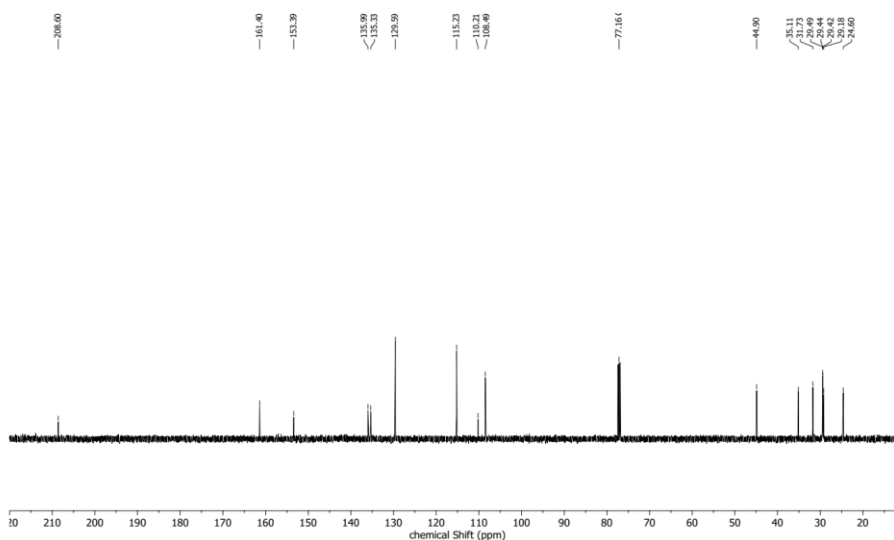


**Figure S6:  $^{13}\text{C}$  NMR ( $\text{CD}_3\text{OD}$  50 MHz) spectrum of compound 2 (Malabaricone B).**

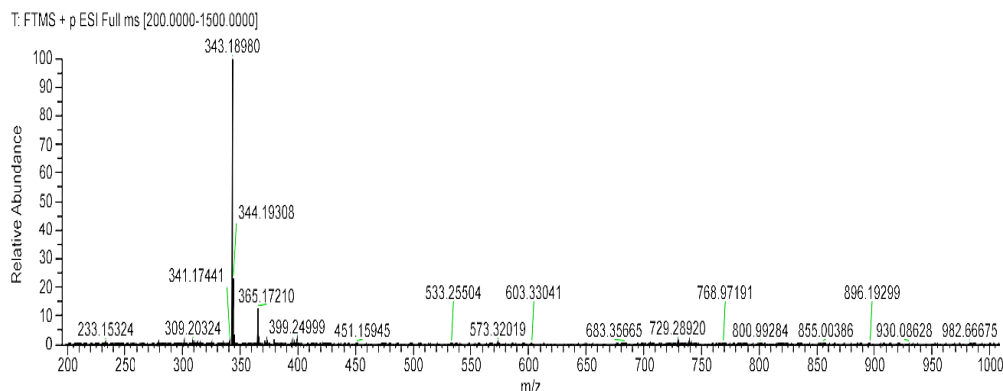


**Figure S7: HRESI (positive mode) mass spectrum of compound 2 (Malabaricone B).**

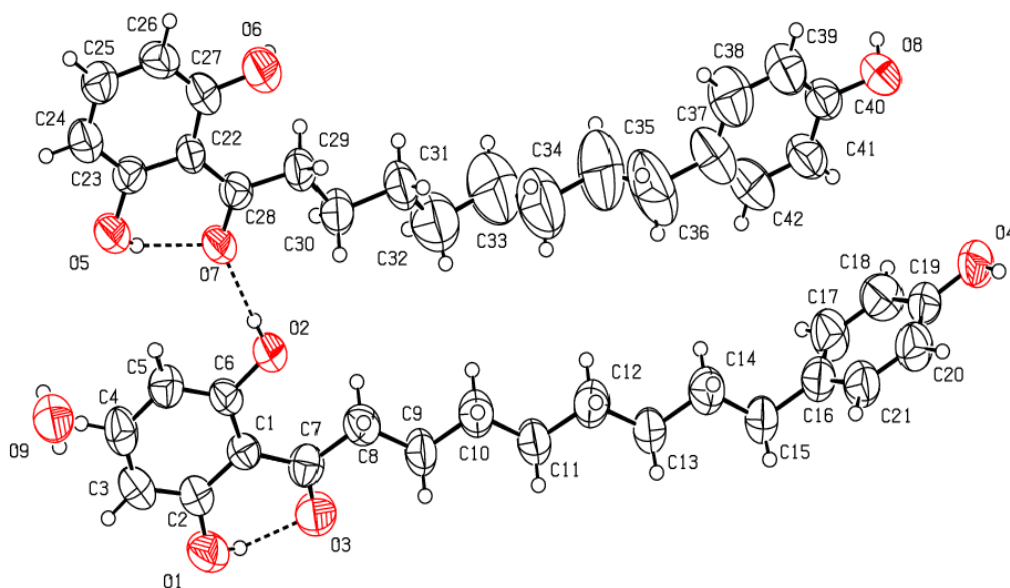


**Figure S8: ORTEP diagram of compound 2 crystallized as twin molecules (Malabaricone B).**

*X-ray crystallographic analysis of compound 2* (Malabaricone B): Crystals of compound **2** were obtained from a mixture ethyl acetate and hexane.

*Crystal data of compound 2:* symmetry cell setting monoclinic (0.500 x 0.080 x 0.080) mm<sup>3</sup>, space group name P2<sub>1</sub>/n. Unit cell dimensions: a = 5.378 (2) Å, α = 90°; b = 17.027(4) Å, β = 90.65 (2)°; c = 42.401 (7) Å, γ = 90°; cell volume, V = 3882.5 (18) Å<sup>3</sup>; cell formula unit, Z = 4; cell measurement temperature 293(2) K; cell reflection used 14535; cell measurement θ<sub>min</sub> 2.578; cell measurement θ<sub>max</sub> 25.348°; crystal description colourless needle shaped crystal; crystal diffraction density, d<sub>x</sub> = 1.202 Mg/m<sup>3</sup>; diffraction ambient temperature 293 (2) K; diffraction radiation wave length, λ = 0.71073 Å; diffraction radiation type MoKα; diffraction radiation source fine focus sealed tube; diffraction radiation monochromator graphite. Absorption coefficient 0.083 mm<sup>-1</sup>; experimental crystal F (000) = 1512; θ range for data collection 2.578 to 25.348°. Limiting index ranges: 4 ≤ h ≤ 6, -20 ≤ k ≤ 15, -40 ≤ l ≤ 51; independent

reflections measured = 6963 [R(int.) = 0.1550]. Completeness to θ = 25.242°, 97.5%. Absorption correction: semi-empirical from equivalents. Maximum and minimum transmission = 0.993 and 0.960. The structure was solved by direct methods and refined by full-matrix least-squares on F<sup>2</sup>. Final R indices [I > 2σ(I)]: R1 = 0.0937, wR2 = 0.1844; extinction coefficient 0.0014 (4); largest difference peak and hole 0.270 and -0.259 e. Å<sup>-3</sup>.

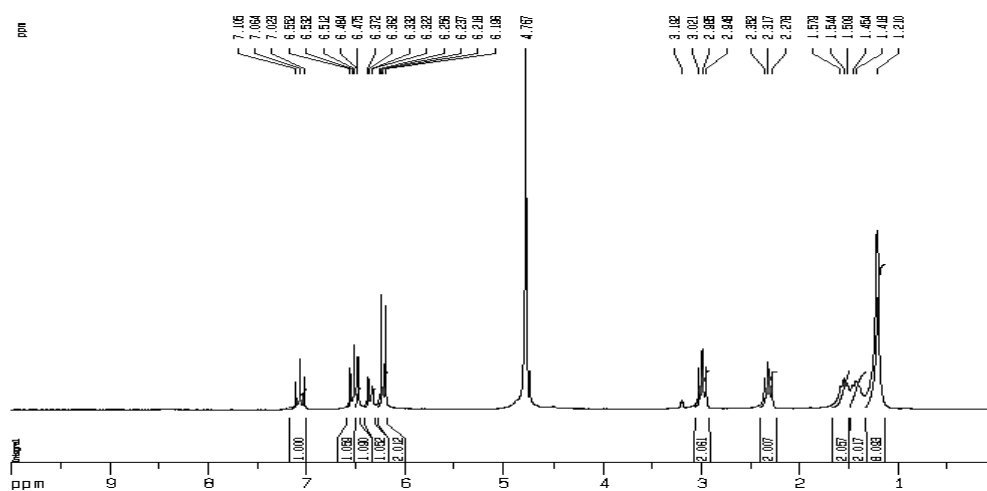


Figure S9:  $^1\text{H}$  NMR ( $\text{CD}_3\text{OD}$ , 200 MHz) spectrum of compound 3 (Malabaricone C).

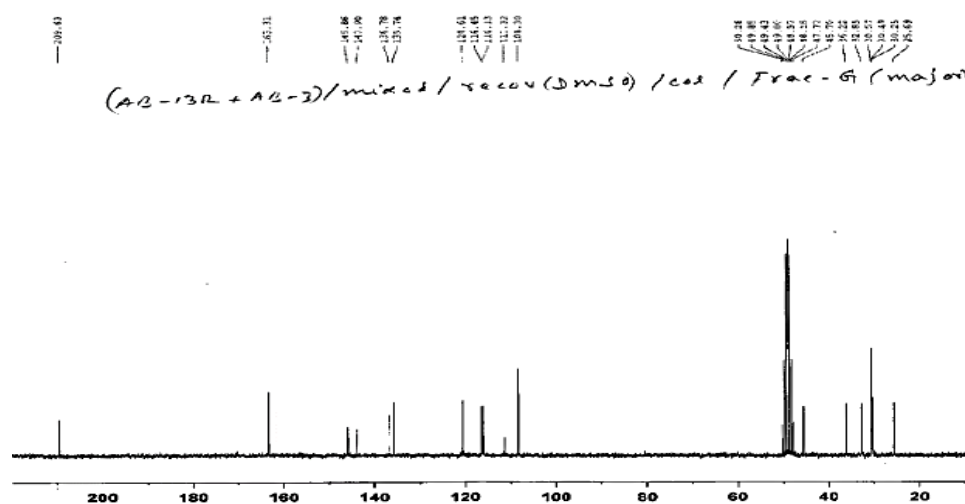


Figure S10:  $^{13}\text{C}$  NMR ( $\text{CD}_3\text{OD}$ , 50 MHz) spectrum of compound 3 (Malabaricone C).

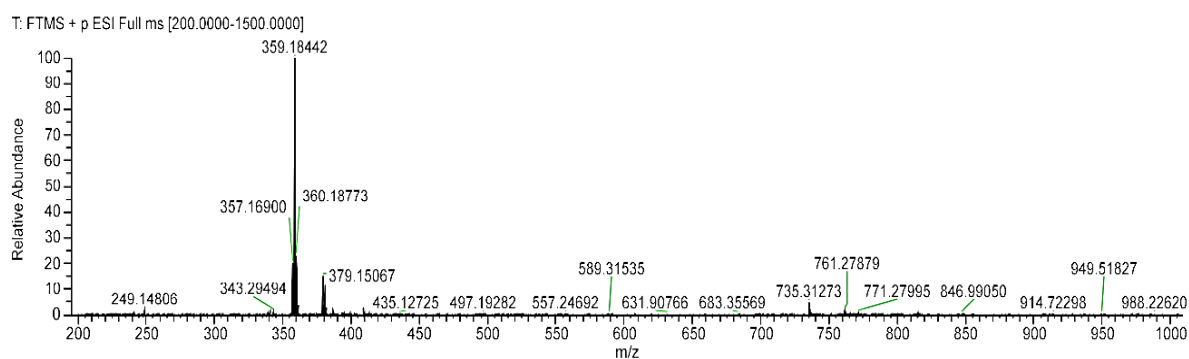
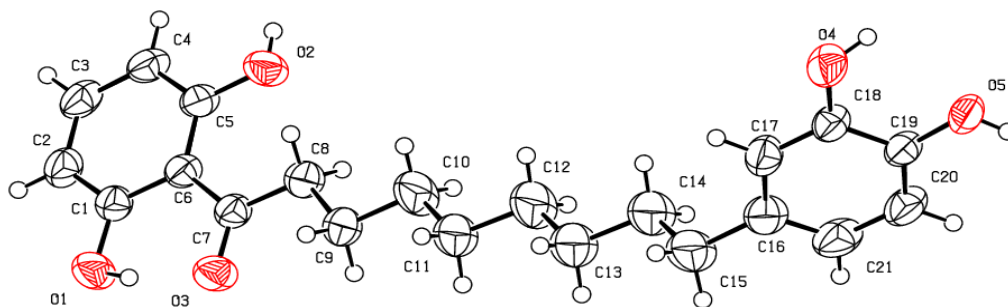


Figure S11: HRESI-MS (positive mode) spectrum of compound 3 (Malabaricone C).





**Figure S12: ORTEP diagram of compound 3 (Malabaricone C).**

*X-ray Crystallographic Analysis of compound 3 (Malabaricone C):* Crystals of compound **3** were obtained in a mixture ethyl acetate and hexane.

*Crystal data of compound 3:* symmetry cell setting orthorhombic; size of crystals used for diffraction study (0.5 x 0.25 x 0.20 mm<sup>3</sup>); symmetry space group P2<sub>1</sub>2<sub>1</sub>2<sub>1</sub>; space group name P 2ac 2ab. Unit cell dimensions: a = 5.4549 (6),  $\alpha$  = 90°, b = 9.176 (1),  $\beta$  = 90°, c = 40.718(3),  $\gamma$  = 90°; cell volume, V = 2038.1(3). Unit cell formula, Z = 4; cell measurement temperature, T 299 (2); cell measurement reflections used = 25; cell measurement  $\theta_{\min}$  = 5.81, cell measurement  $\theta_{\max}$  = 20.19; crystal description long needle dark yellow in color;

crystal density diffraction, d = 1.227 Mg m<sup>-3</sup>; diffraction ambient temperature, T 299 (2)°; diffraction radiation wave length,  $\lambda$  = 1.54180; diffraction radiation type CuK $\alpha$ ; diffraction radiation source fine focus sealed tube; diffraction radiation monochromator graphite. 3822 independent reflections were measured and 3323 reflections were observed with [R (int.) = 0.032]. Completeness to  $\theta$  = 67.0, 100%. The structure was solved by direct methods and refined by a full matrix least square on F<sup>2</sup>. Final R indices [I > 2 $\sigma$  (I)]: R1 = 0.048, wR2 = 0.137; s = 1.04; extinction coefficient 0.0035(6), largest difference peak and hole = 0.20 and -0.21 e.Å<sup>-3</sup>.

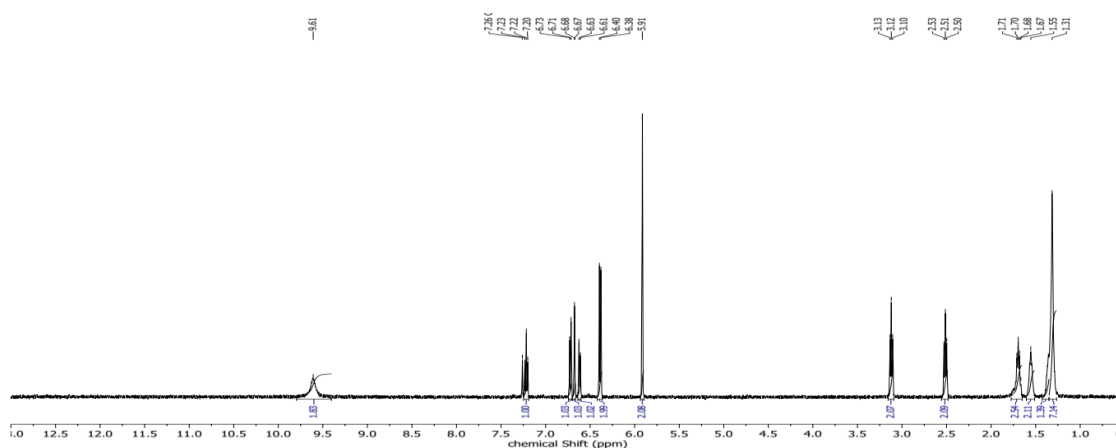


**Figure S13: <sup>1</sup>H NMR (CD<sub>3</sub>OD, 200 MHz) spectrum of compound 4 (Malabaricone D).**

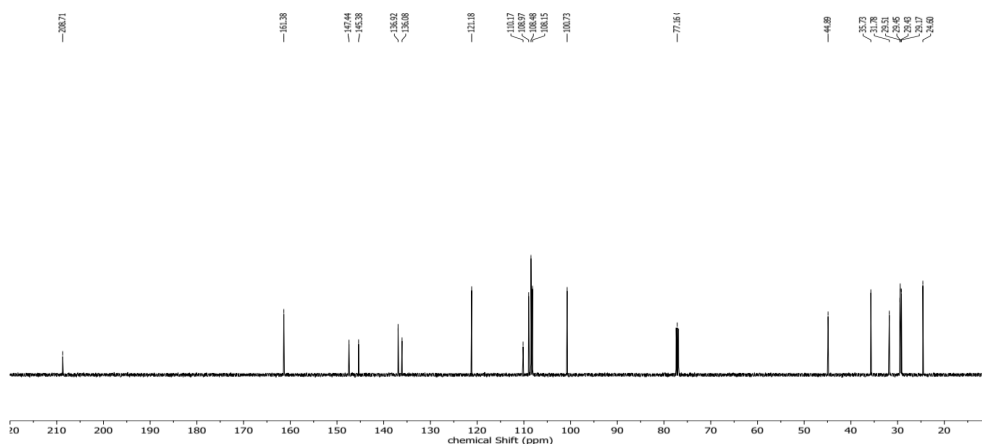


**Figure S14: <sup>13</sup>C NMR (CD<sub>3</sub>OD, 50 MHz) spectrum of compound 4 (Malabaricone D).**

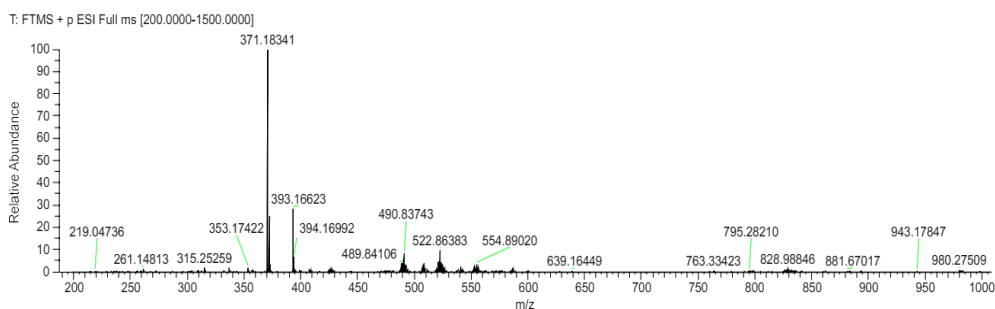


Figure S15: HRESI-MS of compound 4 [found  $MH^+$  = 371.1834] (Malabaricone D).

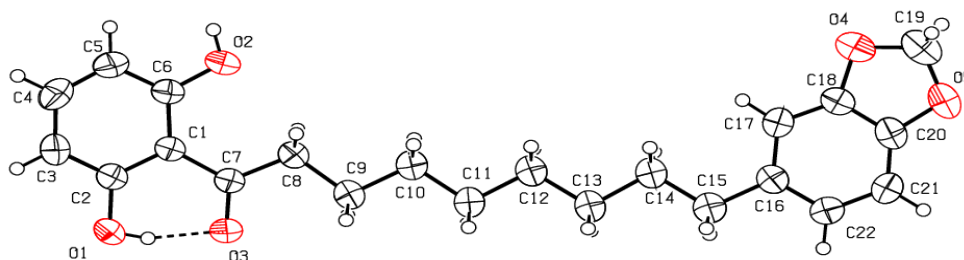


Figure S16: ORTEP diagram compound 4 (Malabaricone D) recorded from TU, Darmstadt, Germany.

*X-ray crystallographic analysis of compound 4* (Malabaricone D): It was crystallized from a mixture of binary solvent system using ethyl acetate and hexane in ratio 20:80 v/v by slow evaporation method.

*Crystal data of compound 4* (Malabaricone D): Empirical formula of molecule  $C_{22}H_{26}O_5$ ; formula weight of it 370.43; crystal description: prism shaped yellow color; size of crystal used for diffraction study (0.480 x 0.440 x 0.240 mm<sup>3</sup>); symmetry cell setting: monoclinic; symmetry space group name:  $P2_1/c$ . Unit cell dimensions:  $a = 12.837$  (2) Å,  $\alpha = 90^\circ$ ,  $b = 14.178$  (2) Å,  $\beta = 98.28$  (2)°,  $c = 10.815$  (2) Å,  $\gamma = 90^\circ$ ; cell volume,  $V = 1947.8$  (6) Å<sup>3</sup>. Unit cell formula,  $Z = 4$ ; cell measurement temperature,  $T$  293(2) °K; cell measurement reflections collected = 7321;  $\theta$  range for data collection: 2.716 to 25.347°. cell measurement  $\theta_{min}$ : 2.716°, cell measurement  $\theta_{max}$ : 25.347°; Index ranges  $-15 \leq h \leq 14$ ,  $-17 \leq k \leq 15$ ,  $-12 \leq l \leq 13$ ; crystal density diffraction,  $d = 1.227$  Mg/m<sup>3</sup>; diffraction ambient temperature,  $T$  293

(2)°; diffraction radiation wave length,  $\lambda = 0.71073$  Å; source of diffraction radiation type MoK $\alpha$ ; diffraction radiation source fine focus sealed tube; diffraction radiation monochromator graphite; diffraction measurement device type: Oxford Diffraction Xcalibur (TM) Single Crystal X-ray Diffractometer with Sapphire CCD Detector. Total reflections were collected 3747 [ $R(int.) = 0.0515$ ]; independent reflections were measured with 3542 [ $R(int.) = 0.0590$ ];  $R$  indices (all data):  $R1 = 0.1127$ ,  $wR2 = 0.2302$ . Maximum and minimum transmission were 0.979 and 0.959; Completeness to  $\theta = 25.242^\circ$ , 99.4%. Method used for absorption correction is semi-empirical from equivalents. Structure was solved by direct methods and refined by a full matrix least square on  $F^2$ . Goodness-of-fit on  $F^2$  1.008 Final  $R$  indices [ $I > 2\sigma(I)$ ]:  $R1 = 0.0669$ ,  $wR2 = 0.1773$ ; restrain refined,  $s = 1.063$ ; extinction coefficient 0.00079(17), largest difference peak and hole 0.205 & -0.316 e.Å<sup>-3</sup>.

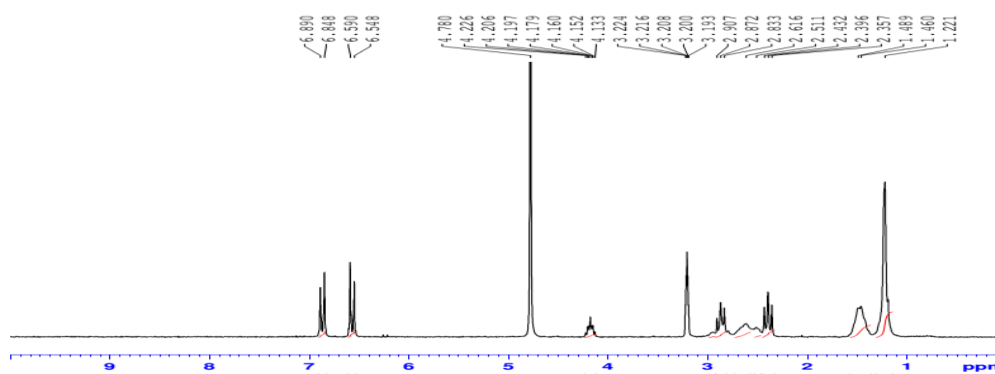


Figure S17: <sup>1</sup>H NMR ( $CD_3COCD_3$ , 200 MHz) spectrum of compound 5 (Promalabaricone B).

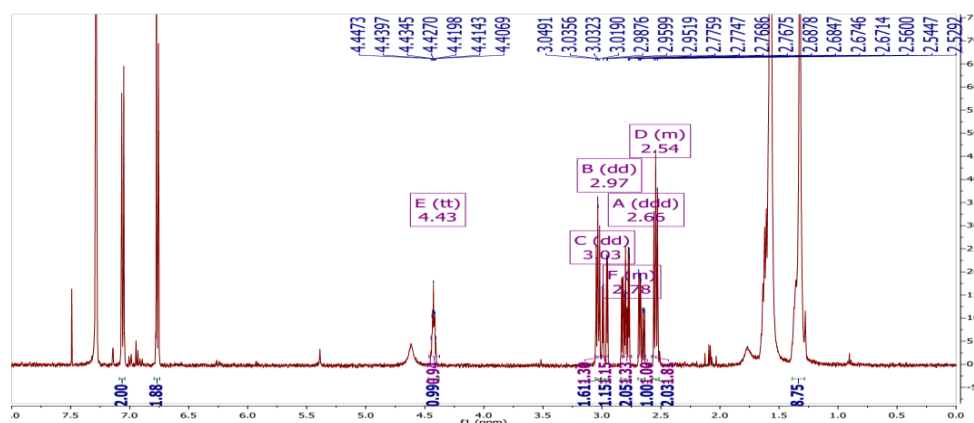


Figure S18:  $^1\text{H}$  NMR ( $\text{CDCl}_3$ , 400 MHz) spectrum of compound 5 (Promalabaricone B), recorded from VT, USA.

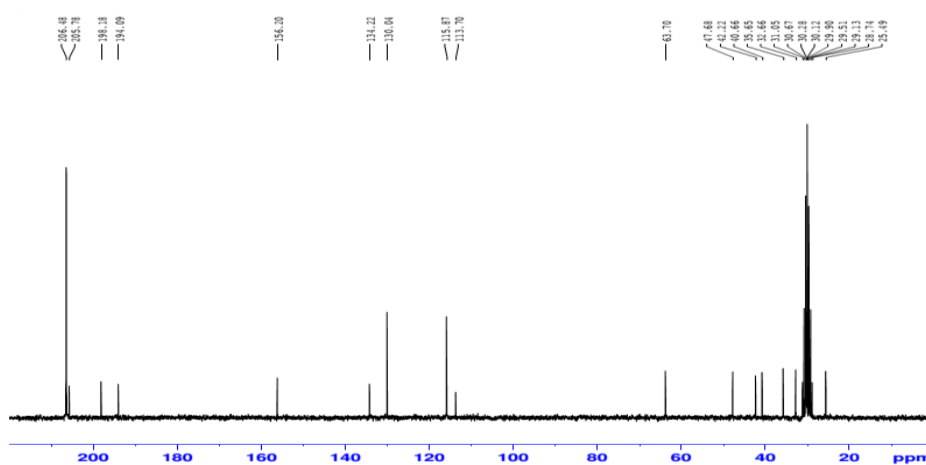


Figure S19:  $^{13}\text{C}$  NMR ( $\text{CD}_3\text{COCD}_3$ , 50 MHz) spectrum of compound 5 (Promalabaricone B)

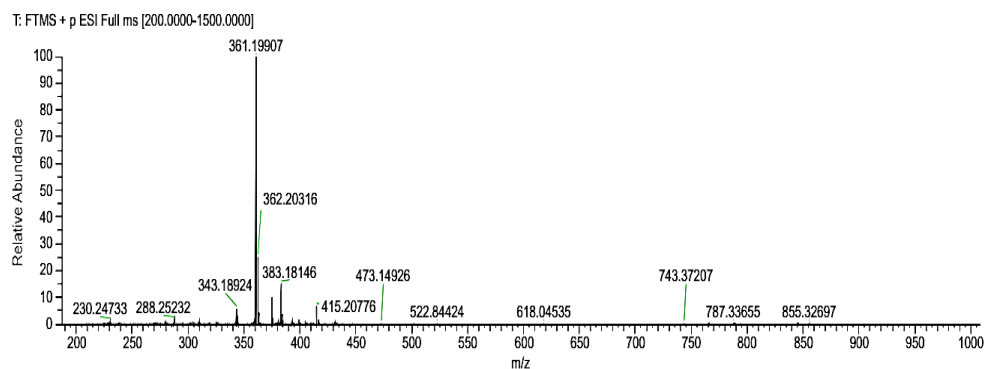


Figure S20: HR-ESI mass spectrum of compound 5 (Promalabaricone B) recorded from OSU, USA.

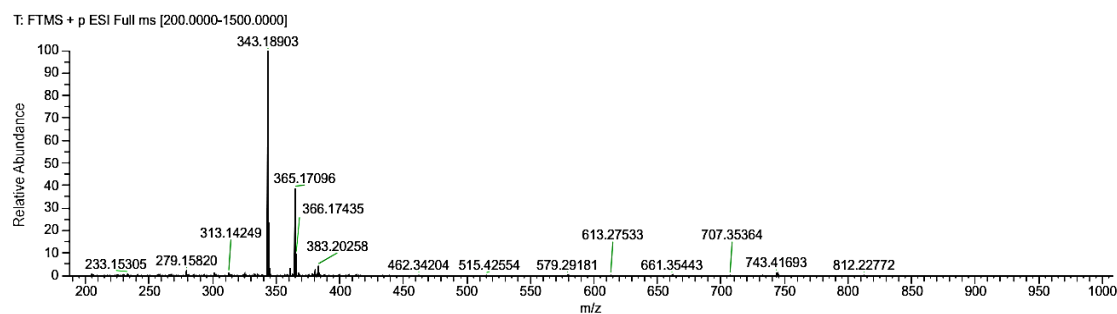


Figure S21: HR-ESI Mass Spectrum of compound 5  $[\text{M}-\text{H}_2\text{O}]$  (Promalabaricone B) recorded from OSU, USA.



*Crystal data of compound 5* (Promalabaricone B): orthorhombic crystal (0.28 x 0.12 x 0.20 mm<sup>3</sup>); space group name Pbc<sub>a</sub>. Unit cell dimension measured: a = 15.690 (2) Å, α = 90°; b = 5.382 (1) Å, β = 90°; c = 48.546 (5) Å, γ = 90°; cell volume, V = 4099 (10) Å<sup>3</sup>. Unit cell formula, Z = 8; absorption coefficient, μ = 0.09 mm<sup>-1</sup>. Experimental crystal F (000) = 1632. Number of independent reflections were measured = 8537 and number of independent reflections observed 3753 [R(int.) = 0.1072]. Completeness to θ = 25.24, 98.8%.

Crystal density diffraction,  $d_x = 1.226 \text{ Mg/m}^3$ . Absorption correction: semi-empirical equivalents; crystal description orthorhombic, crystal colour -colourless. Diffraction radiation ambient temperature 293(2) K; diffraction radiation wavelength,  $\lambda = 0.71073 \text{ \AA}$ ; diffraction radiation type MoK $\alpha$ ; diffraction radiation source fine focus sealed tube; diffraction radiation monochromator graphite;  $\theta$  range for data collection  $2.596$  to  $25.346^\circ$ . Limiting indices  $-18 \leq h \leq 14$ ,  $-4 \leq k \leq 6$ ,  $-23 \leq l \leq 58$ ; Maximum and minimum transmission:  $0.998$  and  $0.976$ ; Structure was solved by direct methods refined by full-matrix least-squares on  $F^2$ . Final R indices [ $I > 2\sigma(I)$ ]:  $R1 = 0.1406$ ,  $wR2 = 0.3301$ ; R indices (all data)  $R1 = 0.3407$ ,  $wR2 = 0.4505$ ; largest difference peak and hole  $0.656$  and  $-0.268 \text{ e. \AA}^{-3}$ .





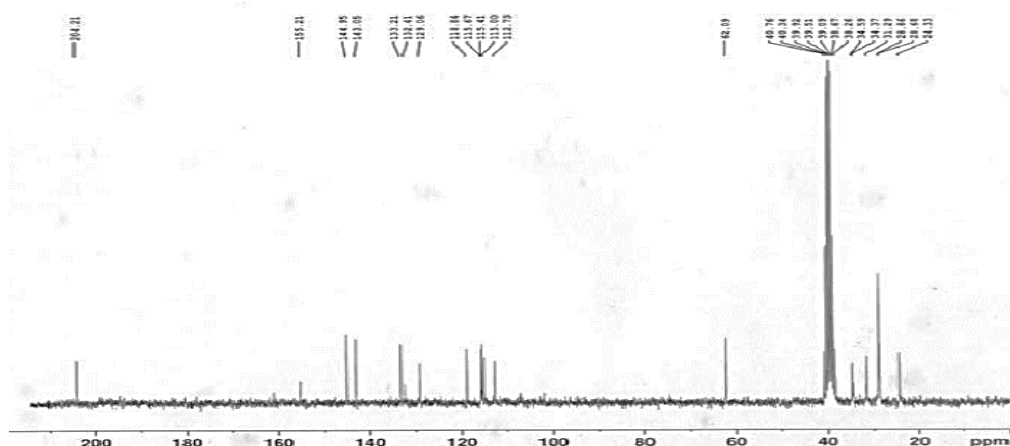


Figure S25:  $^{13}\text{C}$  NMR ( $\text{CD}_3\text{OD}$ , 50 MHz) spectrum of compound 6 (Promalabaricone B).

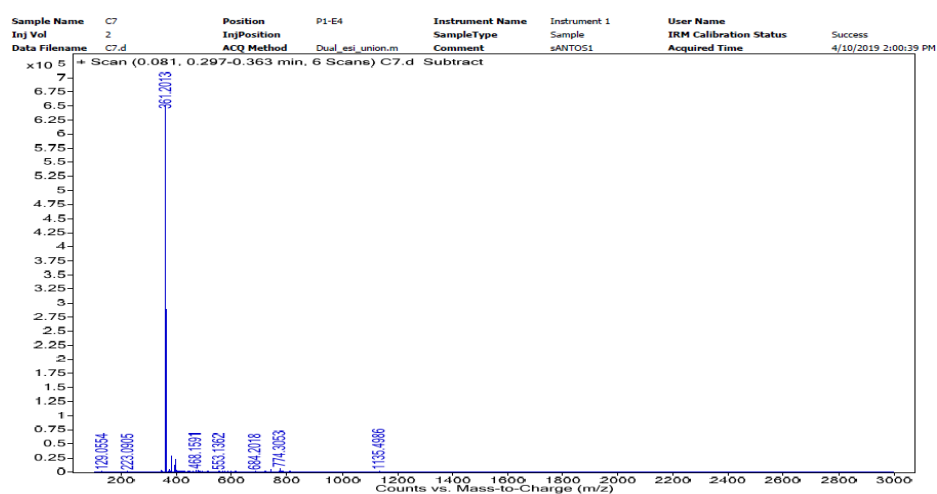


Figure S26: HRESI-MS spectrum of compound 6 [one water molecule eliminated ( $\text{M}^+ - \text{H}_2\text{O}$ )] (Promalabaricone B).

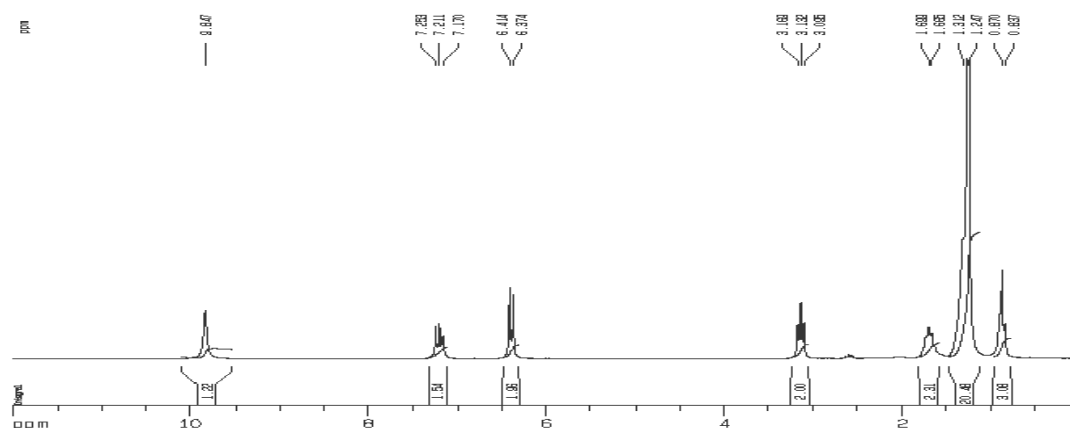


Figure S27:  $^1\text{H}$  NMR ( $\text{CDCl}_3$ , 200 MHz) spectrum of compound 7 (Acyl phenol).

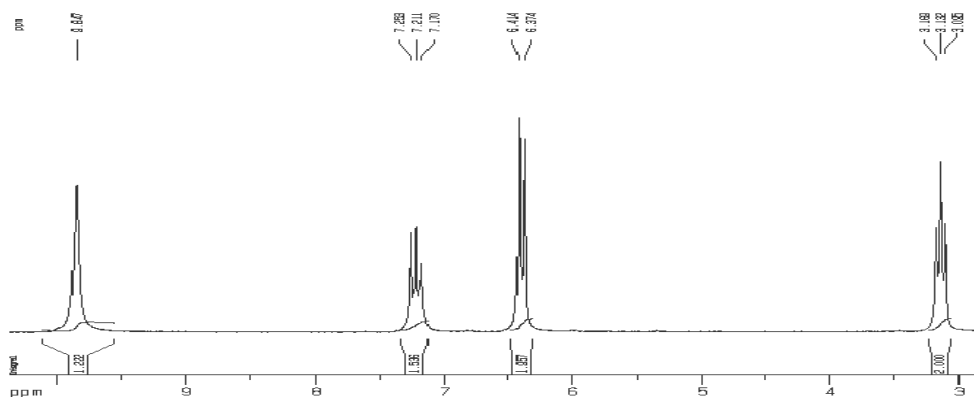


Figure S28:  $^1\text{H}$  NMR ( $\text{CDCl}_3$ , 200 MHz) spectrum of compound 7 (Acyl phenol).

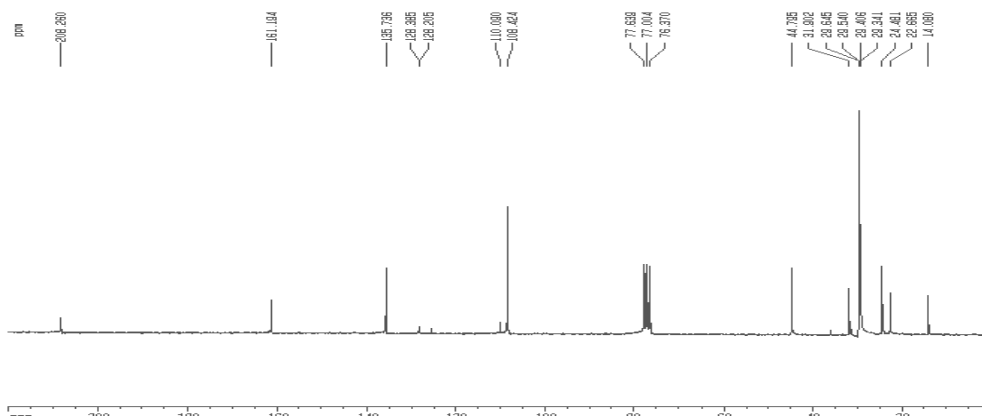


Figure S29:  $^{13}\text{C}$  NMR ( $\text{CDCl}_3$ , 50 MHz) spectrum of compound 7 (Acyl phenol).

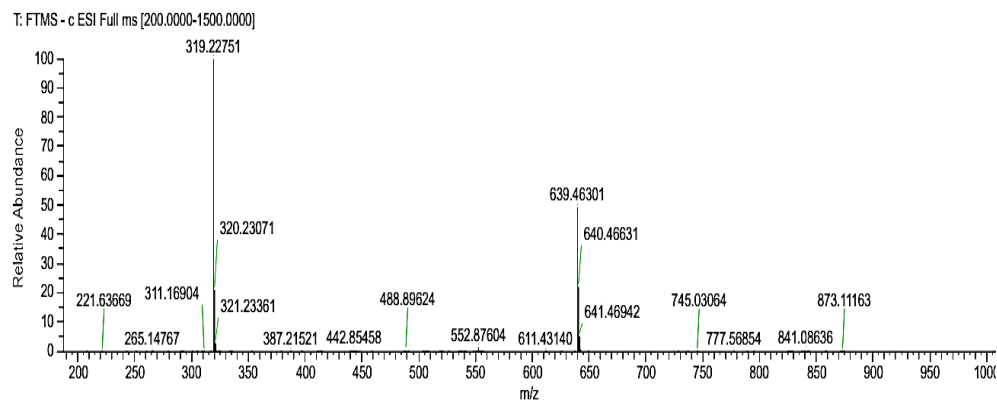


Figure S30: HRESI-MS (negative mode) of compound 7 (Acyl phenol).

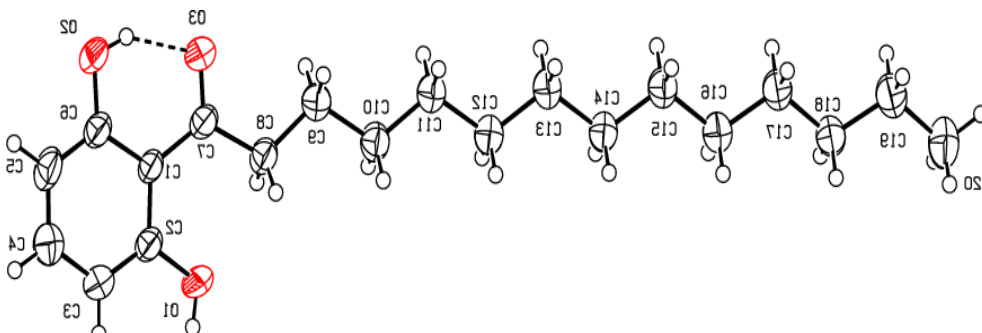
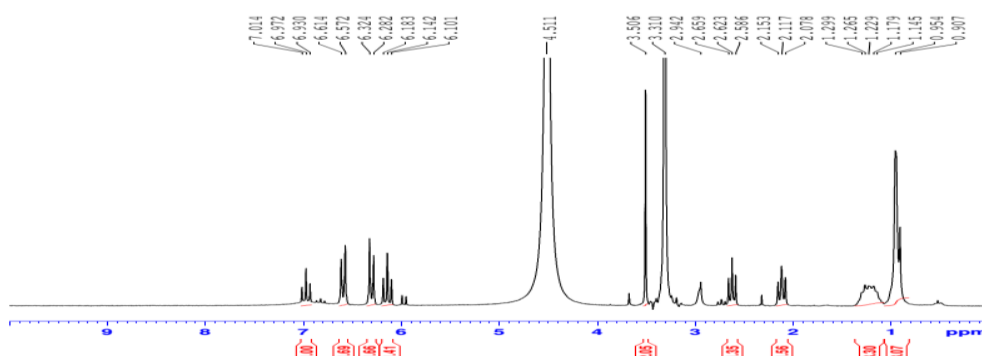


Figure S31: ORTEP diagram of compound 7 (Acyl phenol) (recorded from TU, Darmstadt, Germany).

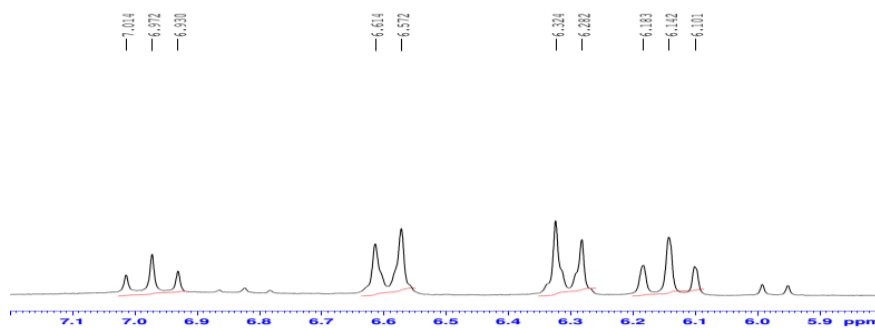
**X-ray Crystallographic Analysis of compound 7** (Acyl phenol): It was crystallized from a mixture of ethyl acetate and hexane in ratio 10:90 v/v by slow evaporation method at room temperature.

**Crystal data of compound 7** (Acyl, phenol): monoclinic crystal (0.50 x 0.12 x 0.08 mm); space group name P 2<sub>1</sub>/c; crystal description long needle; crystal colour pale yellow. Unit cell dimensions: a = 4.2047 (6) Å,  $\alpha$  = 90°; b = 34.146 (4) Å,  $\beta$  = 97.67 (1) °; c = 13.347 (3) Å,  $\gamma$  = 90°; cell volume, V = 1899.1 (6) Å<sup>3</sup>. Unit cell formula, Z = 4; cell measurement temperature 293 (2) K; cell measurement  $\theta_{\min}$  = 2.84 deg. Cell measurement  $\theta_{\max}$  = 25.34 deg. Crystal density diffraction,  $d_x$  = 1.121 Mg/m<sup>3</sup>. Diffraction temperature 293K; diffraction radiation wave

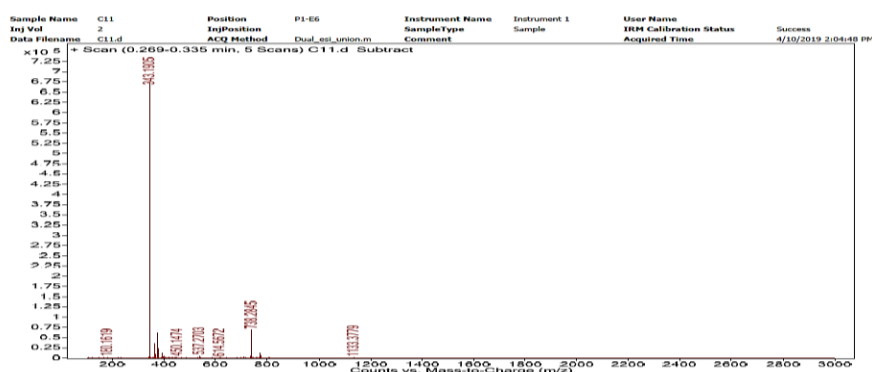
length,  $\lambda$  = 0.71073 Å; diffraction radiation type MoK $\alpha$ . Diffraction radiation source fine focus sealed tube. Absorption coefficient,  $\mu$  = 0.07 mm<sup>-1</sup>. Total number of independent reflections were measured 6324, number of independent reflections 3396 and number of independent reflections were observed [R (int.) = 0.0252] = 2217. Completeness to theta = 25.34; 98.3%. Absorption correction: semi-empirical from equivalents. Maximum and minimum transmission = 0.9942 and 0.9643. The structure was solved by direct methods and refined by full-matrix least-squares on F<sup>2</sup>. Final R indices [F<sup>2</sup> > 2 $\sigma$  (F<sup>2</sup>)], R1 = 0.0857, wR (F<sup>2</sup>) = 0.160; R indices (all data) R1 = 0.1364, wR2 = 0.1604. Largest difference peak and hole 0.19 and -0.16 e. Å<sup>-3</sup>.



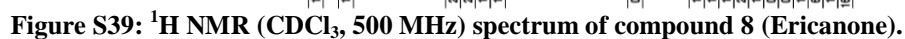
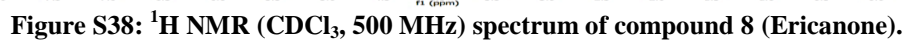
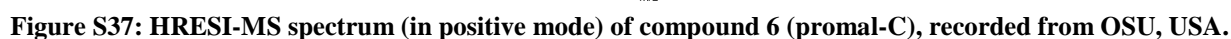
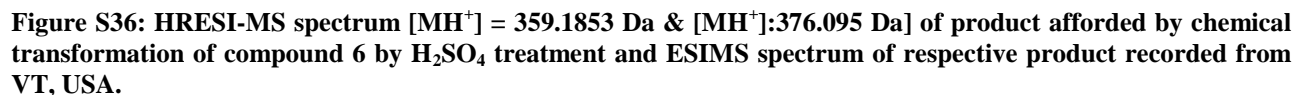
**Figure S32:** <sup>1</sup>H NMR (CD<sub>3</sub>OD, 200 MHz) spectrum of crude product yielded on treatment with H<sub>2</sub>SO<sub>4</sub> (dehydration reaction: promalabaricone B treated with concentrated H<sub>2</sub>SO<sub>4</sub> produced malabaricone B.



**Figure S33:** Expansion of <sup>1</sup>H NMR (CD<sub>3</sub>OD, 200 MHz) spectrum of crude product yielded on treatment with H<sub>2</sub>SO<sub>4</sub> (dehydration reaction: promalabaricone B treated with concentrated H<sub>2</sub>SO<sub>4</sub> produced malabaricone B.



**Figure S35:** HRESI-MS [MH<sup>+</sup> = 343.1905 Da] of product yielded by chemical transformation of compound 5 (Promalabaricone B) to 2 (Malabaricone B) on treatment with H<sub>2</sub>SO<sub>4</sub> in MeOH by stirring by 12h).



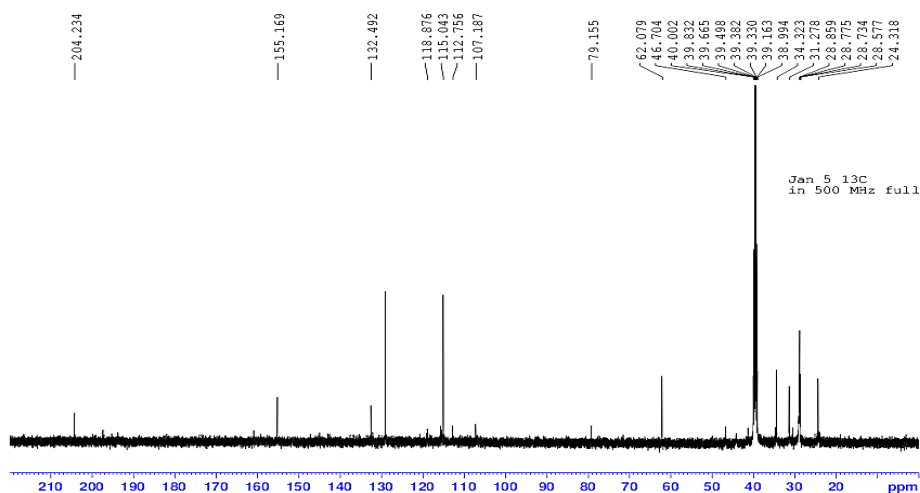


Figure S40:  $^{13}\text{C}$  NMR ( $\text{CDCl}_3$ , 125 MHz) spectrum of compound 8 (Ericanone).

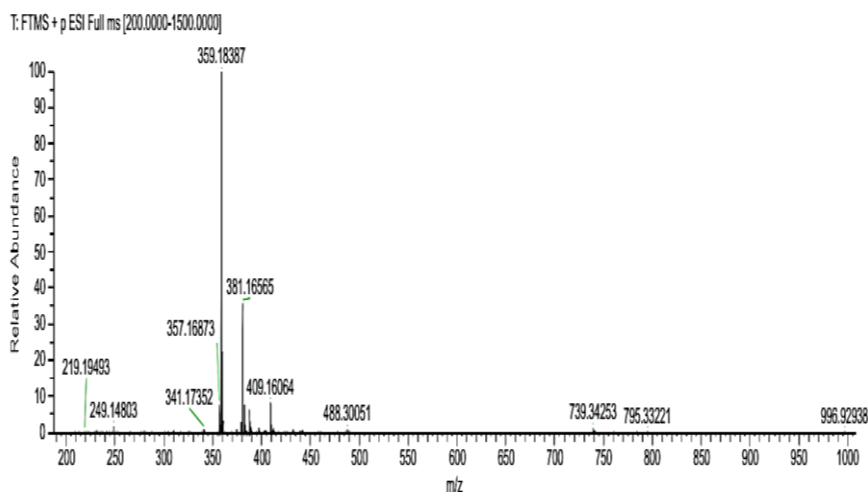


Figure S41: HRESI-MS spectrum (in positive mode) of compound 8 (Ericanone), recorded from OSU, USA.

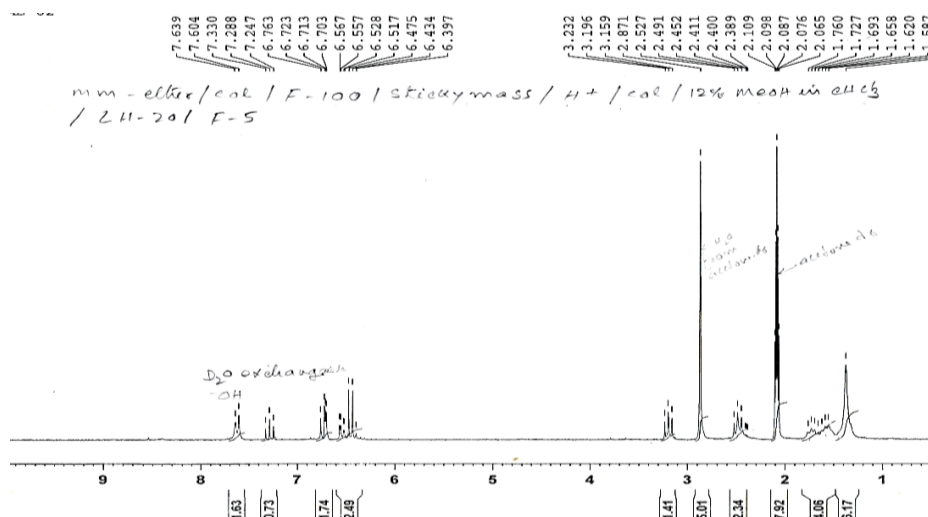


Figure S42:  $^1\text{H}$  NMR ( $\text{CD}_3\text{COCD}_3$ , 200 MHz) of compound 9 (Hydrated malabaricone C).



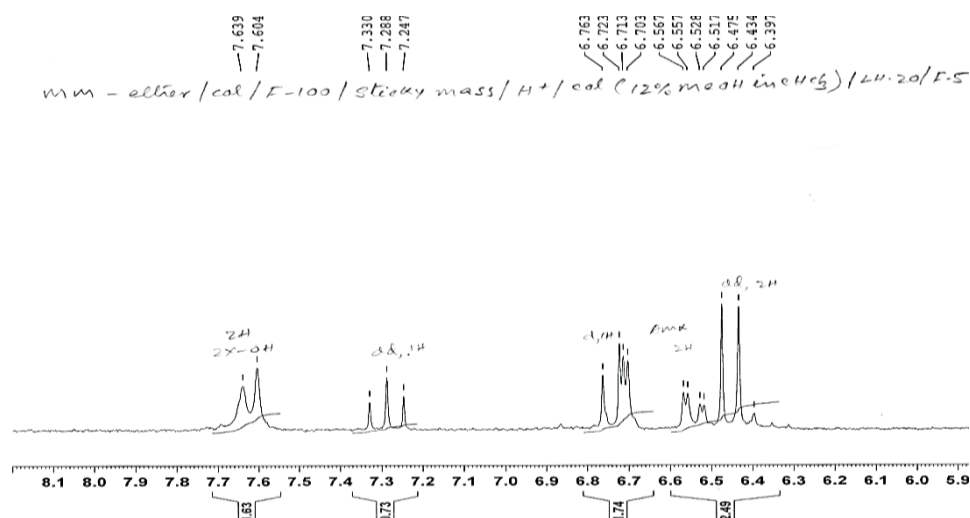


Figure S43: Expansion of  $^1\text{H}$  NMR ( $\text{CD}_3\text{COCD}_3$ , 200 MHz) of compound 9 (Hydrated malabaricone C).

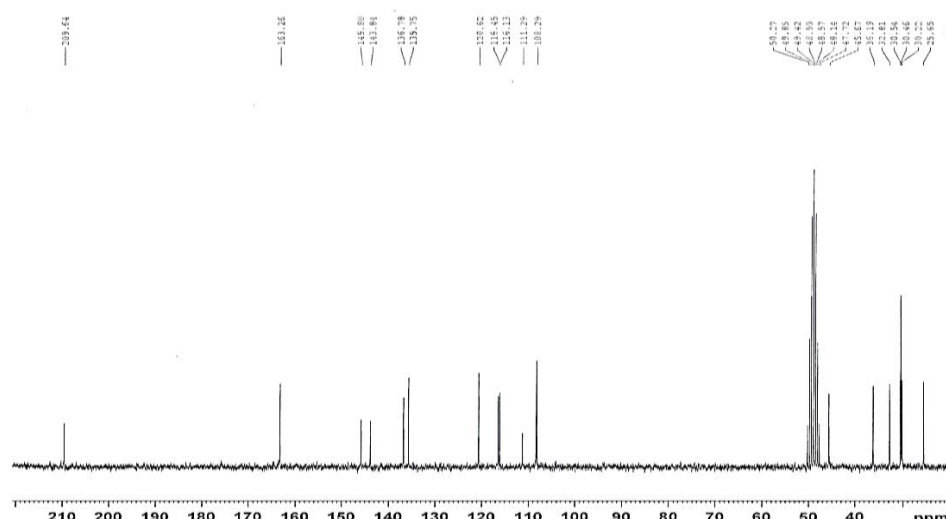


Figure S44:  $^{13}\text{C}$  NMR ( $\text{CD}_3\text{COCD}_3$ , 50 MHz) of compound 9 (Hydrated malabaricone C).

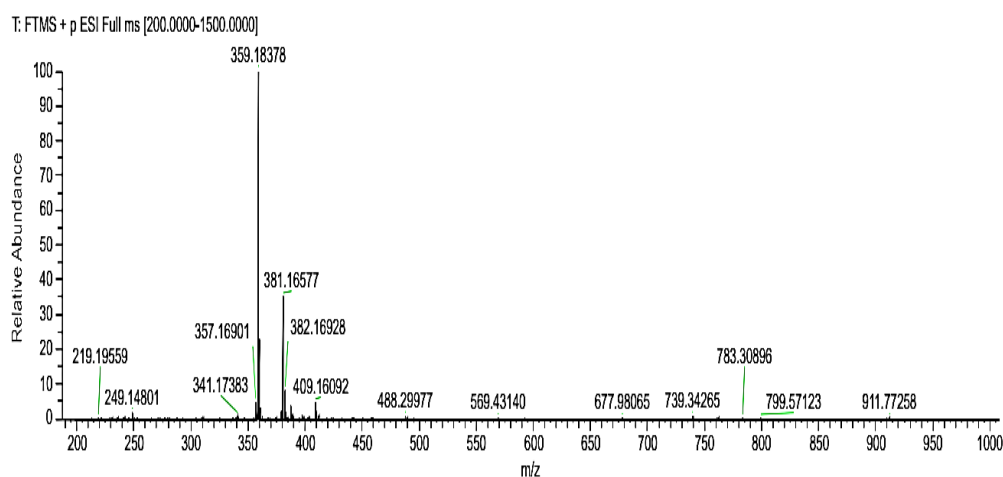
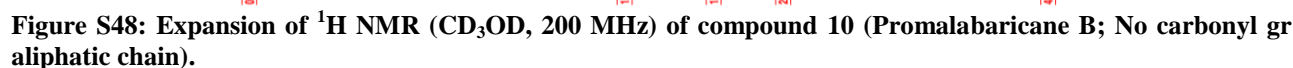


Figure S45: HR-ESIMS spectrum (positive mode) of compound 9 (Hydrated malabaricone C).



(2) $^{\circ}$ ; diffraction radiation wave length,  $\lambda = 1.54180$ ; diffraction radiation type CuK $\alpha$ ; diffraction radiation source fine focus sealed tube; diffraction radiation monochromator graphite. 3822 independent reflections were measured and 3323 reflections were observed with [R (int.) = 0.032]. Completeness to  $\theta = 67.0$ , 100%. The structure was solved by direct methods and refined by a full matrix least square on  $F^2$ . Final R indices [I>2 $\sigma$  (I)]: R1 = 0.048, wR2 = 0.137; s = 1.04; extinction coefficient 0.0035(6), largest difference peak and hole = 0.20 and -0.21 e. $\text{\AA}^{-3}$ .



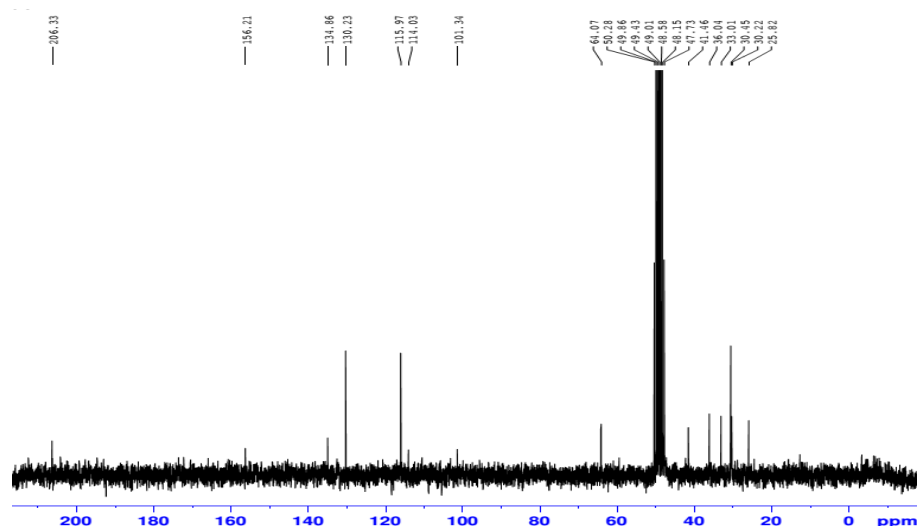


Figure S49:  $^{13}\text{C}$  NMR ( $\text{CD}_3\text{OD}$ , 125MHz) spectrum of compound 10 (Promalabaricane B; No carbonyl group aliphatic chain).

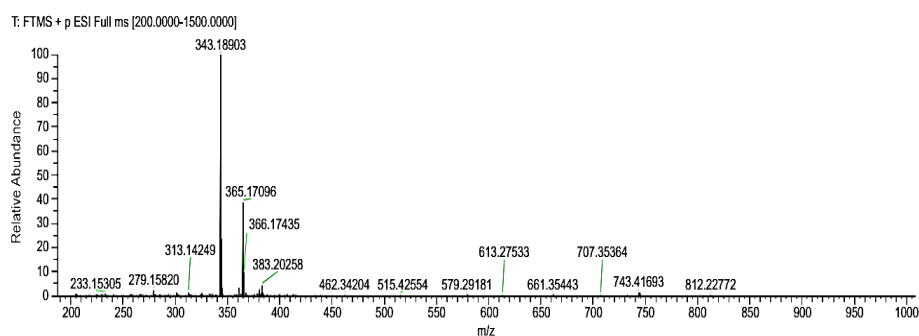


Figure S50: HRESI-MS (positive mode) of compound 10 (Promalabaricane B No carbonyl group aliphatic chain).

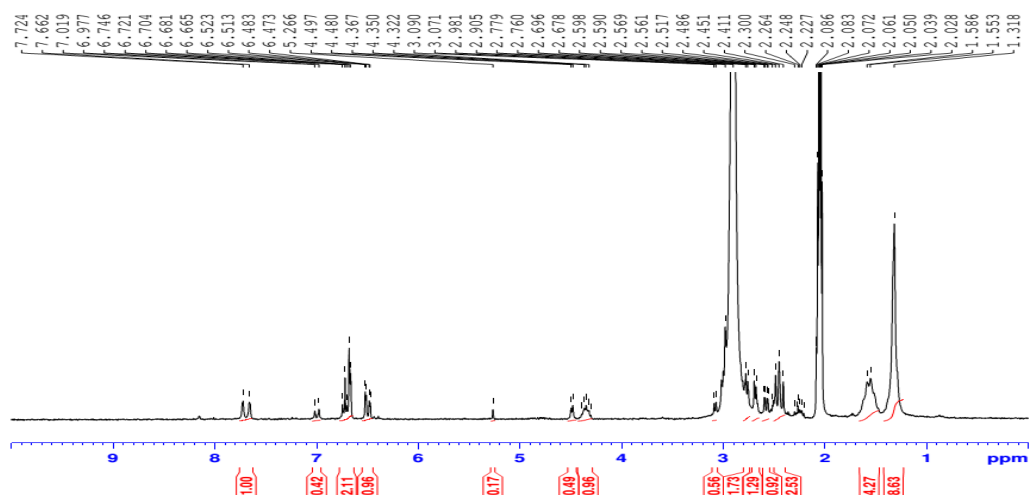


Figure S51:  $^1\text{H}$  NMR ( $\text{CD}_3\text{COCD}_3$ , 200 MHz) of compound 11 (Promalabaricane C. No carbonyl group aliphatic chain).

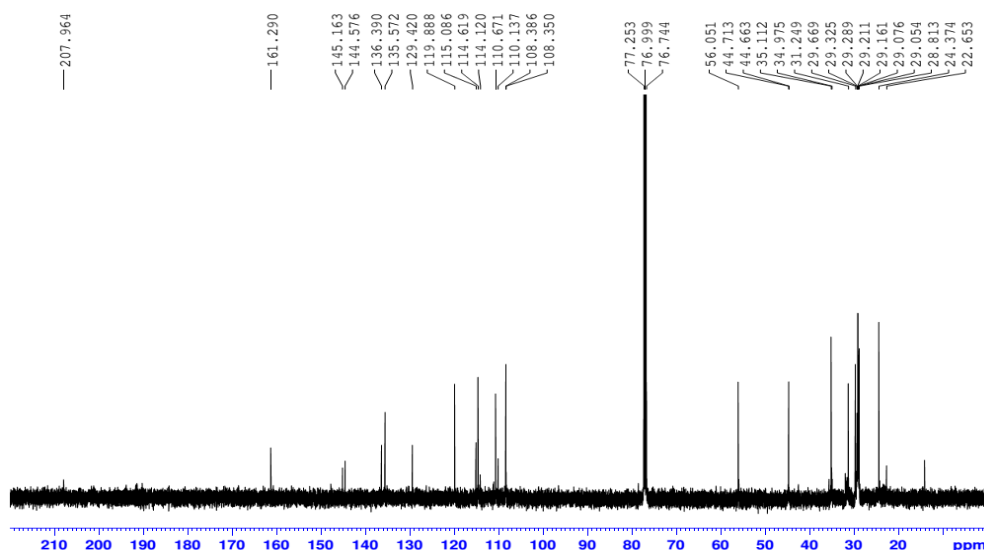


Figure S52:  $^{13}\text{C}$  NMR ( $\text{CDCl}_3$ , 125 MHz) spectrum of compound 11 (Promalabaricane C. No carbonyl group aliphatic chain).

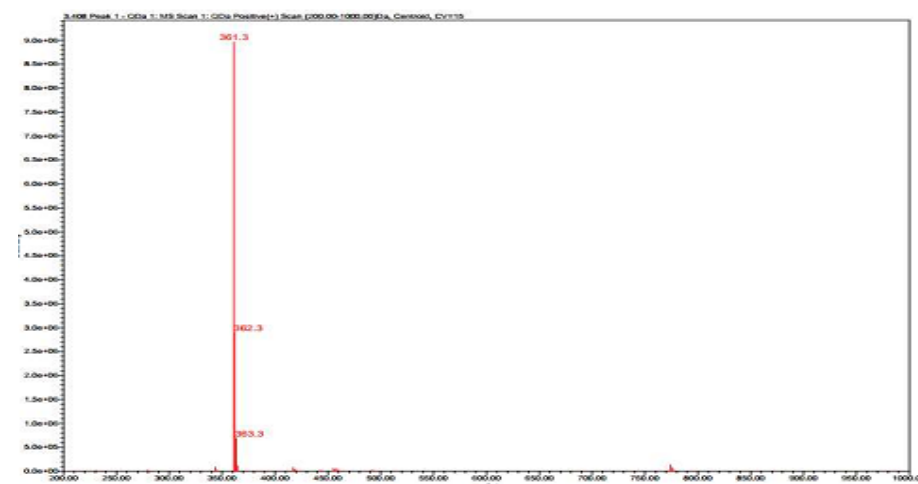


Figure S53: LR-ESIMS spectrum of compound 11 recorded from OSU, USA (Promalabaricane C. No carbonyl group aliphatic chain).

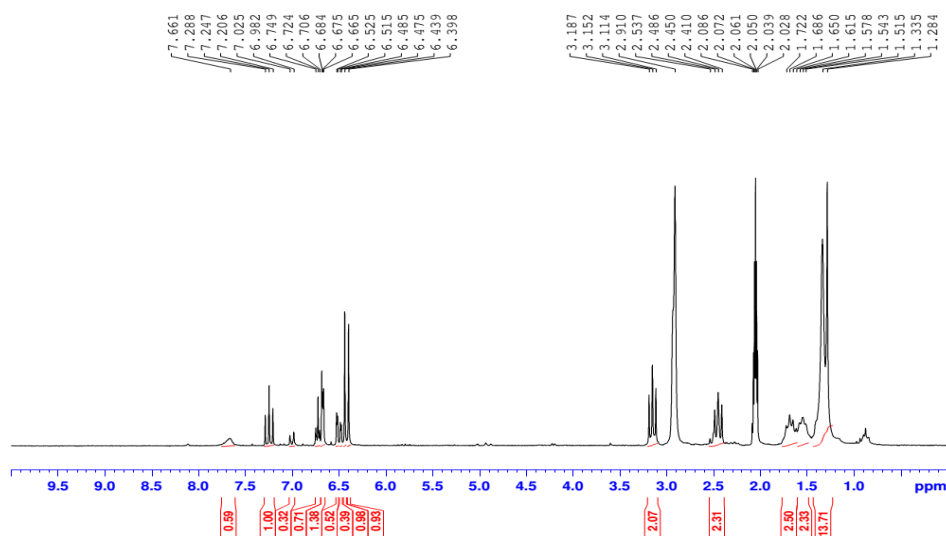


Figure S54:  $^1\text{H}$  NMR ( $\text{CD}_3\text{COCD}_3$ , 200 MHz) of compound 12 (Hydrated malabaricone C) (enrich aglycone yielded on acid hydrolysis glycoside).

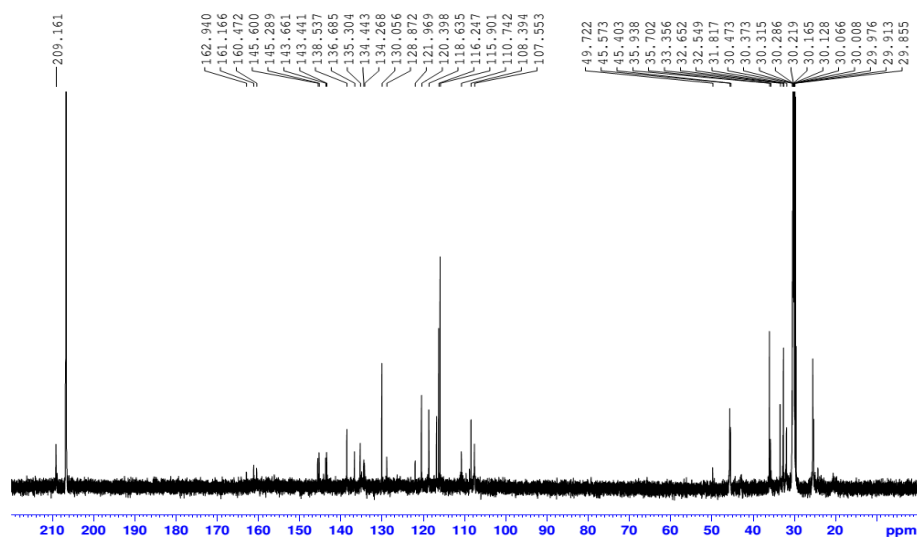


Figure S55:  $^{13}\text{C}$  NMR ( $\text{CD}_3\text{COCD}_3$ , 125 MHz) spectrum of compound 12 (Hydrated malabaricone C) (enrich aglycone yielded on acid hydrolysis of glycoside).

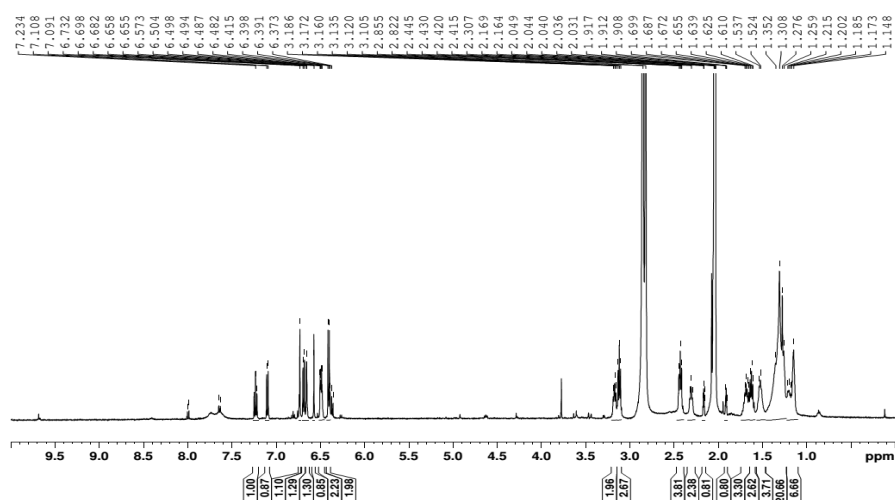
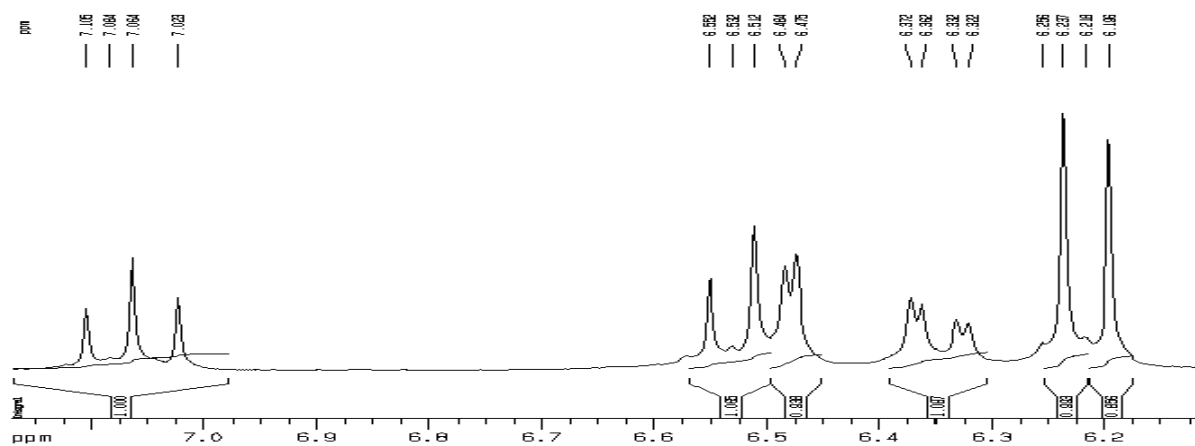


Figure S56:  $^1\text{H}$  NMR spectrum ( $\text{CD}_3\text{COCD}_3$ , 200 MHz) of aglycone yielded on acid hydrolysis of glycoside, a black mug hygroscopic in nature .





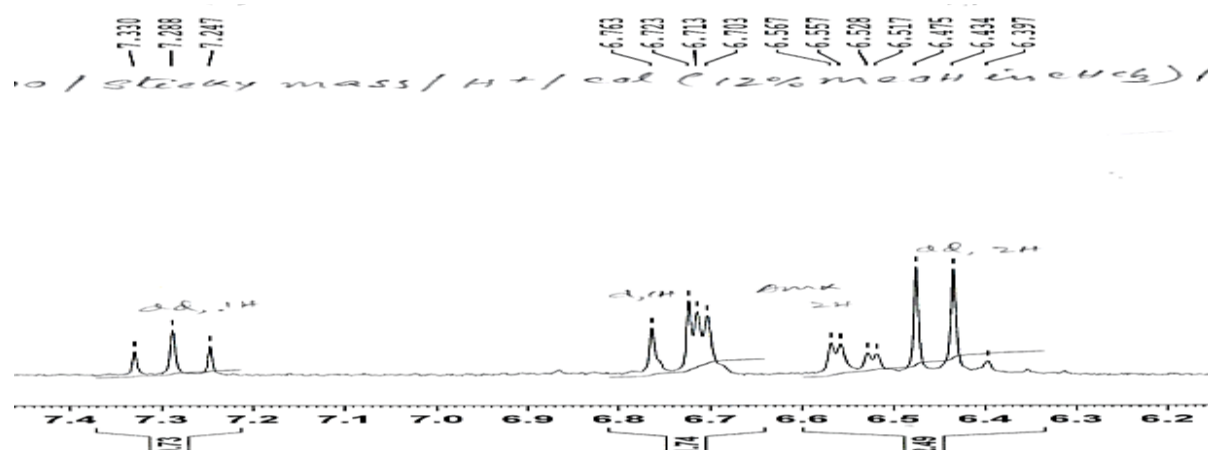


Figure S57: Difference between malabaricone C & hydrated malabaricone C in  $^1\text{H}$  NMR spectra.

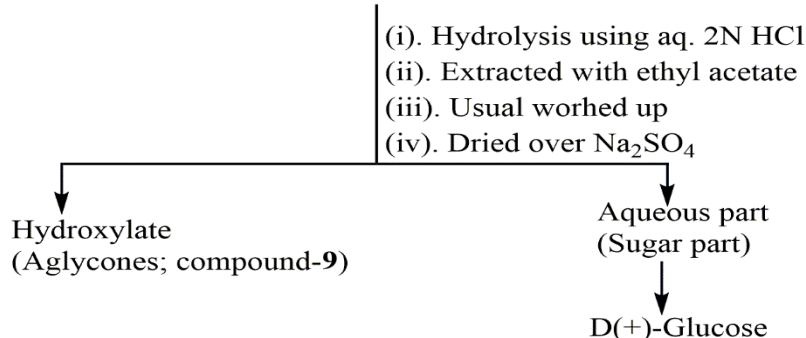
Chart 1: Flow diagram for isolation of secondary metabolites from MeOH extract of *M. malabarica*.

Flow sheet for isolation of secondary metabolites from defatted MeOH extract of fruit rind of *M. malabarica*:

Viscous brown residue (370 gm); subjected to column chromatography over silica gel ( $\text{SiO}_2$  used 5.0 kg; particle size 230-400 mesh, Aldrich, USA); eluted with a binary mixture EtOAc in hexane followed MeOH in  $\text{CHCl}_3$  as solvent system with gradient elution by changing the polarity. Fractions were collected with volume of each aliquot least 500-1000 ml or more volume of aliquots.

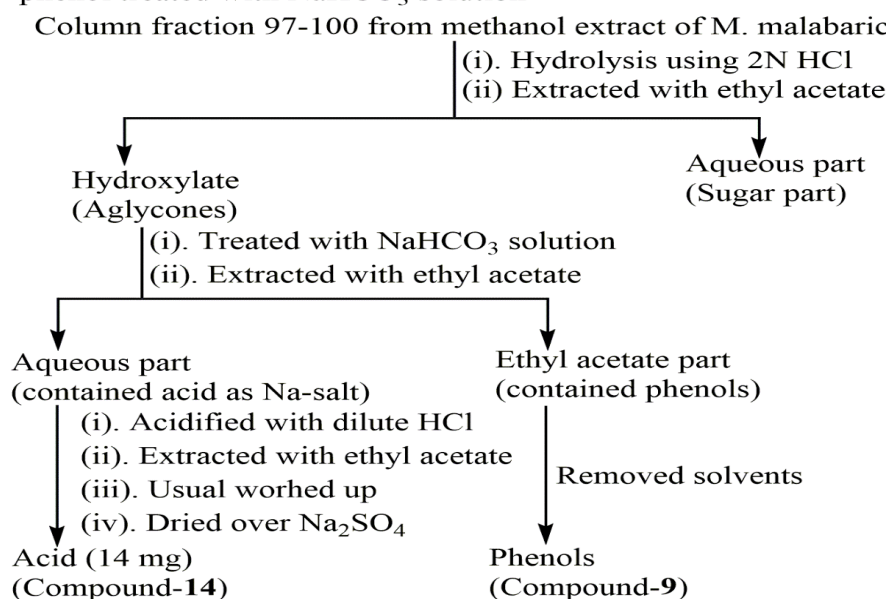
S. no	Col. Frac.	Solvent system used	Yield/Residue	Purification $\text{CC}/\text{SiO}_2/\text{Sep hLH 20}$	Products
1	Frac 1-8	0-15% EtOAc/hexane	Sticky mass	Not done	lipids
2	Frac 9-11	0-5% MeOH in $\text{CHCl}_3$	Crude residue, A (~150 mg)	Sub-fractionated	Compound 7
3	Frac 12-14	5-10% MeOH in $\text{CHCl}_3$	Residue B (1.25 gm)	Sub-fractionated B <sub>5</sub> -B <sub>7</sub>	Compound 1 (1.00 gm)
4	Frac 27-30	10% MeOH in $\text{CHCl}_3$	Crude residue, C (1.5 gm)	Sub-fractionated C <sub>7</sub> -C <sub>11</sub>	Compound 4 (1.25 gm)
5	Frac 34-42	10% MeOH in $\text{CHCl}_3$	Light brown residue, D (1.25 gm)	Sub-fractionated D <sub>7</sub> -D <sub>12</sub>	Compound 2 (2.05 gm)
6	Frac 44-56	10% MeOH in $\text{CHCl}_3$	Pale yellow residue E (13.0 gm)	Sub-fractionated E <sub>7</sub> -E <sub>20</sub>	Compound 3 (11.5 gm)
7	Frac 60-70	15-20% MeOH in $\text{CHCl}_3$	Brown sticky mass F (300 mg)	Sub-fractionated F <sub>4</sub> -F <sub>5</sub>	Compound 8 (100 mg)
9	Frac 71-80	15-20% MeOH in $\text{CHCl}_3$	Light brown sticky mass G (100 mg)	Sub-fractionated G <sub>5</sub> -G <sub>7</sub>	Comp 5 (25) & 6 (14)
10	Frac 81-86	20-25% MeOH in $\text{CHCl}_3$	Colourless solid, H (150 mg)	Sub-fractionated H <sub>3</sub> -H <sub>5</sub> (120 mg)	Prod similar to compounds 5 and 6
11	Frac 87-90	30-35 % MeOH/ $\text{CHCl}_3$	Sticky brown mass, I (500 mg)	Sub-fractionated I <sub>3</sub> -I <sub>5</sub>	Dimers of malabaricones.
12	Frac 91-96	50-70% MeOH/ $\text{CHCl}_3$	Sticky hygroscopic mass, J (50 gm)	Glycosides	Hydrated malabaricone C
13	Frac 97-100	80-100% MeOH/ $\text{CHCl}_3$	Polyphenolic compounds in the form of glycosides	Crude hydroxylate treated with 2% aq. $\text{NaHCO}_3$ to separate acid and phenol	Compounds 9 (25 mg) Compound 12 (10 mg)

**Scheme:** Acid hydrolysis of glycosides to obtain aglycone  
Column fraction 91-96 from methanol extract of *M. malabarica*



**Scheme 1: Scheme for acid hydrolysis of glycoside.**

**Scheme:** Acid hydrolysis of glycosides and separation acid from phenol treated with  $\text{NaHCO}_3$  solution  
Column fraction 97-100 from methanol extract of *M. malabarica*



**Scheme 2: Scheme for acid hydrolysis of glycoside & separation of acid from phenol on treatment with  $\text{NaHCO}_3$  solution**

**Figure S60: Flow diagram for isolation chemical constituents from the fruit rind of *M. malabarica*.**